

Electronic supporting information

Purpurin derivatives as visible-light photosensitizers for 3D-printing and valuable biological applications

*Pauline Sautrot-Ba,¹ Vlasta Brezová,² Jean-Pierre Malval,³ Annalisa Chiapionne,⁴ Louise Breloy,¹ Samir Abbad-Andaloussi,⁵ Davy-Louis Versace*¹*

¹Université Paris-Est Créteil (UPEC), ICMPE–UMR-CNRS 7182, 2-8 rue Henri Dunant, 94320 Thiais, France.

²Slovak University of Technology in Bratislava, Institute of Physical Chemistry and Chemical Physics, Department of Physical Chemistry, Radlinského 9, SK-812 37 Bratislava, Slovak Republic.

³Institut de Chimie des Matériaux de Mulhouse (IS2M)-UMR 7361, 15 rue Jean Starcky - BP 2488, 68057 Mulhouse Cedex, France.

⁴Politecnico di Torino, Dipartimento di Scienza Applicata e Tecnologia, C. so Duca degli Abruzzi 24, 10129 Torino, Italy

⁵Université Paris-Est Créteil (UPEC), Laboratoire Eau, Environnement, Systèmes Urbains (LEESU), UMR-MA 102, 61 avenue Général de Gaulle, 94010 Créteil Cedex, France.

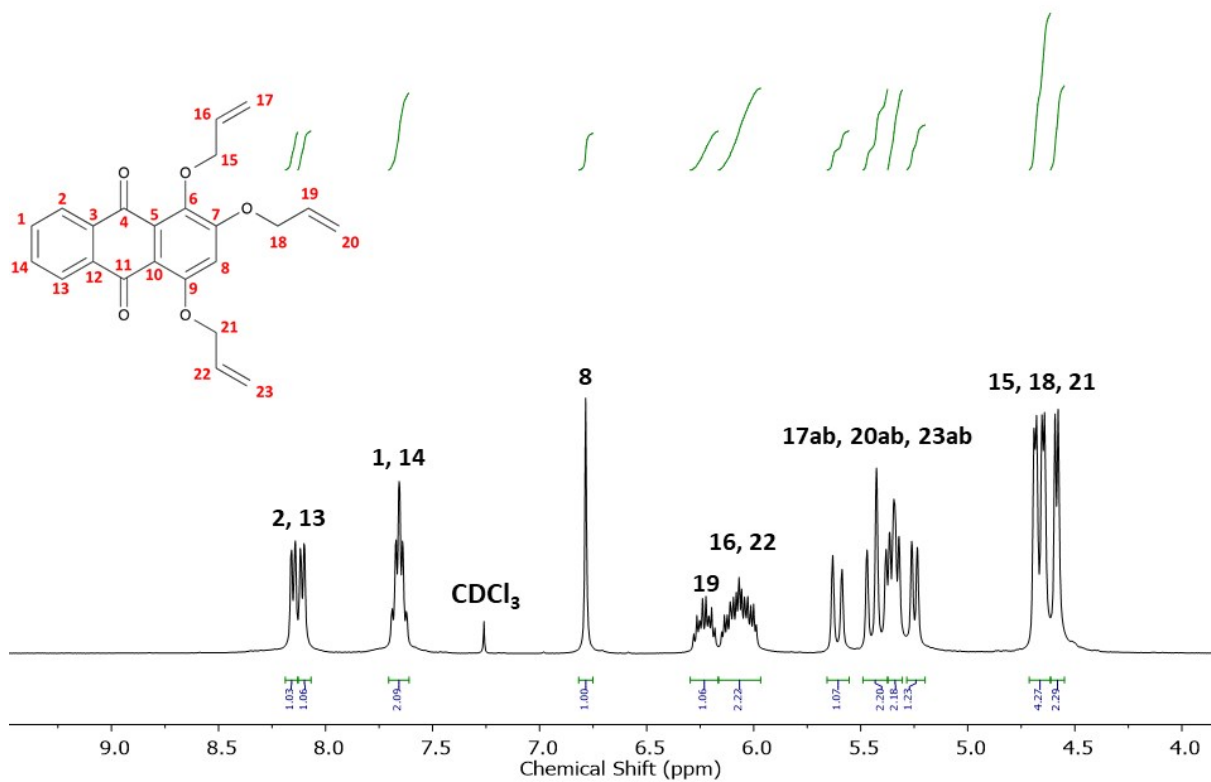


Figure S1. ^1H NMR spectrum of PA in CDCl_3

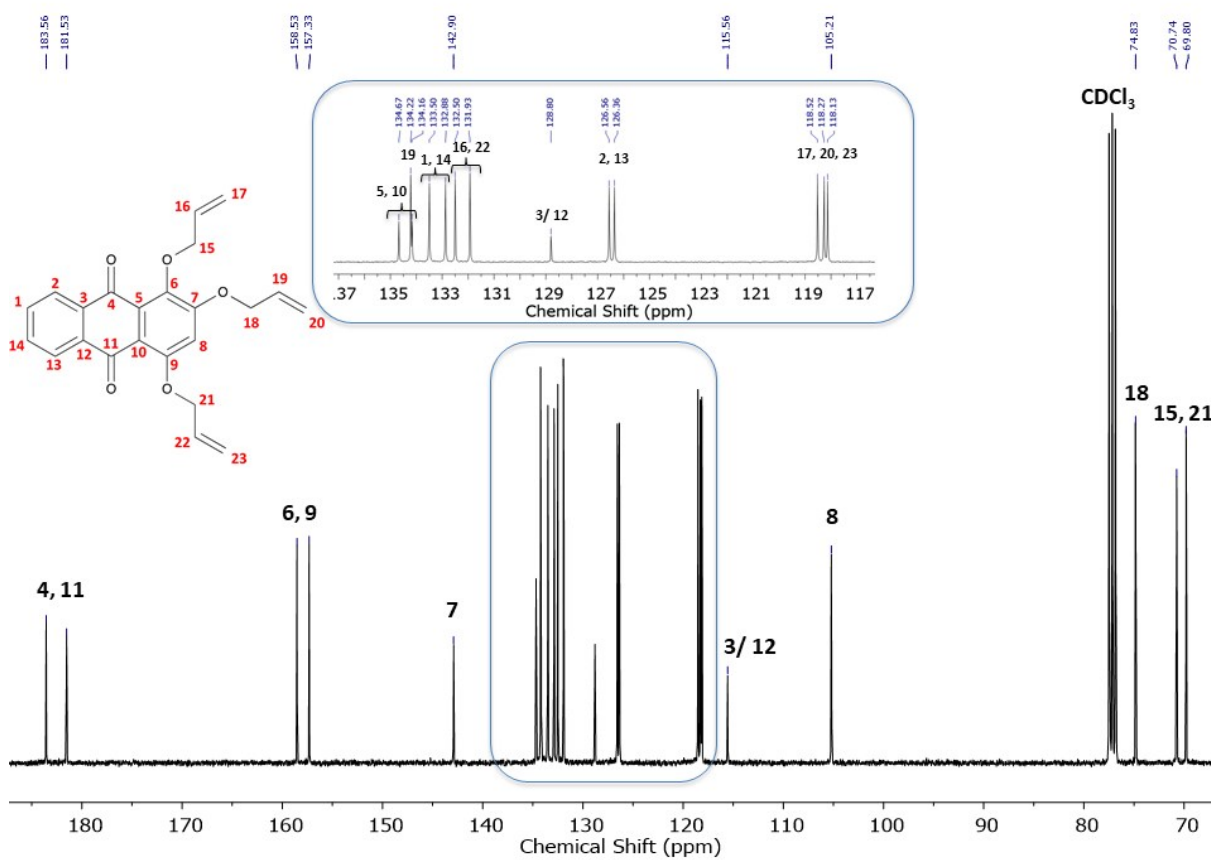


Figure S2. ^{13}C NMR spectrum of PA in CDCl_3

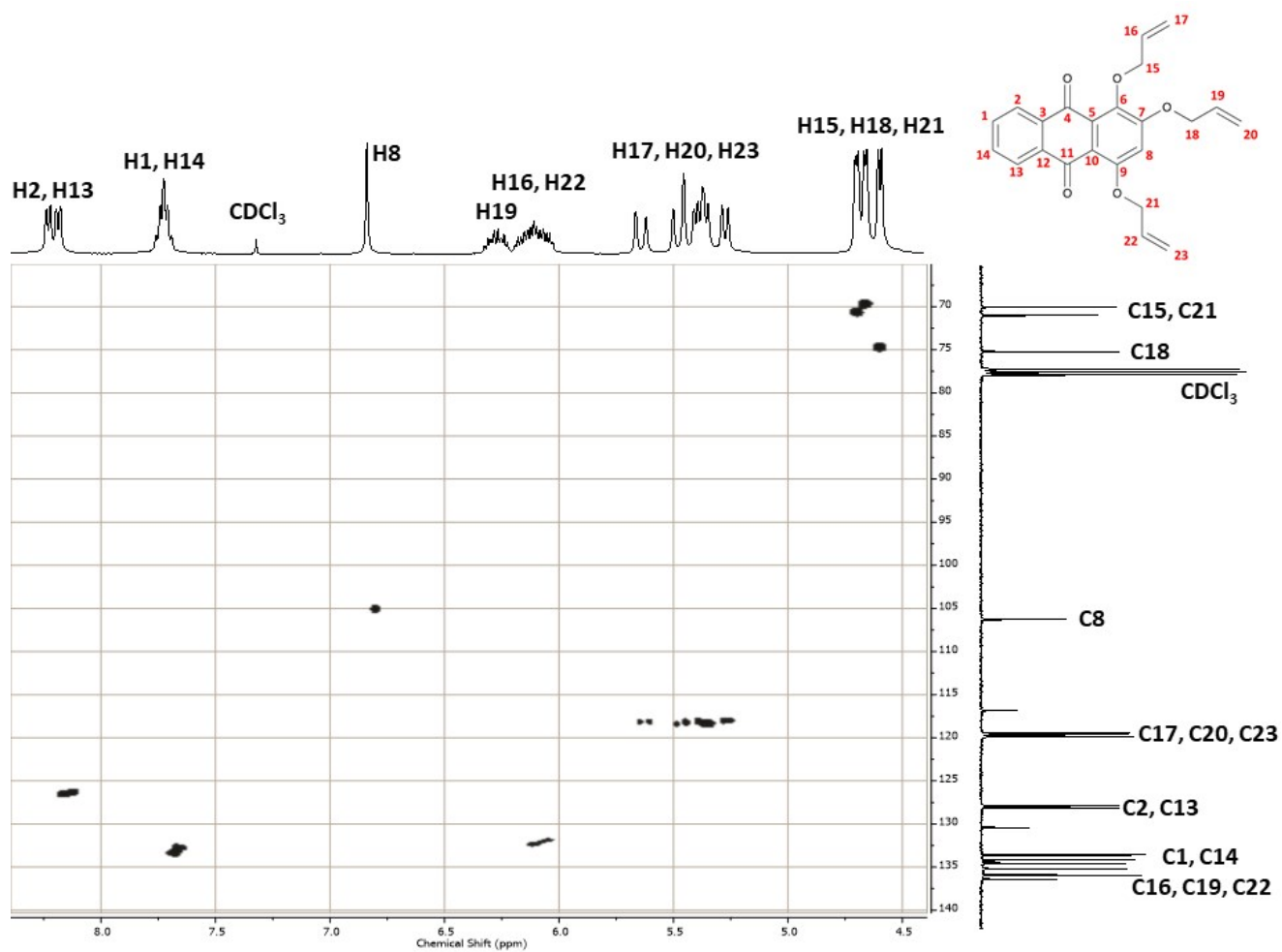


Figure S3. HSQC NMR spectrum of PA in CDCl₃

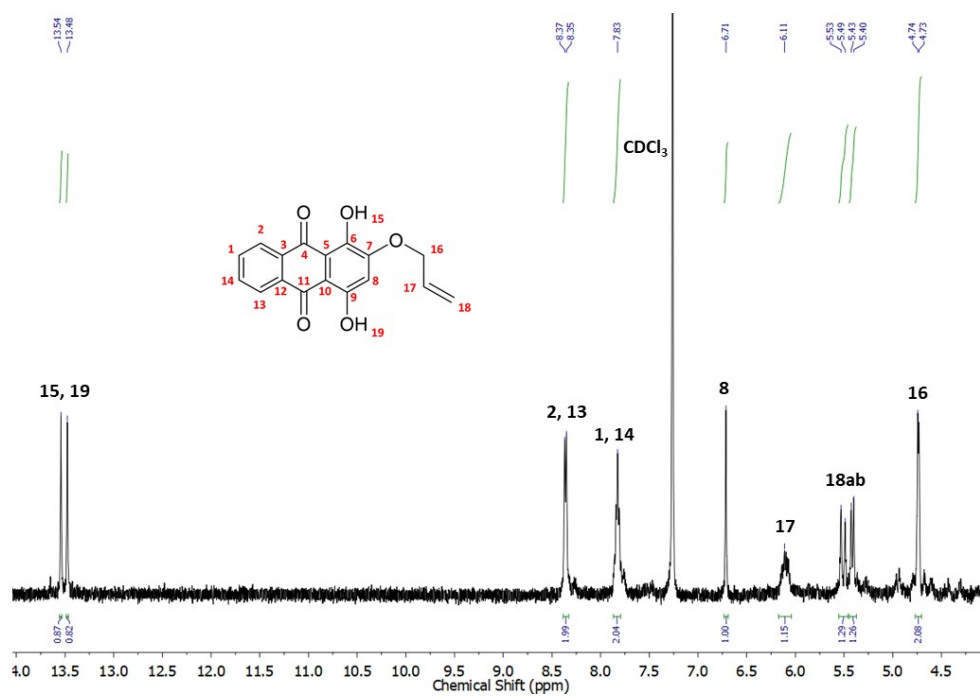


Figure S4. ¹H NMR spectrum of PmA in CDCl₃

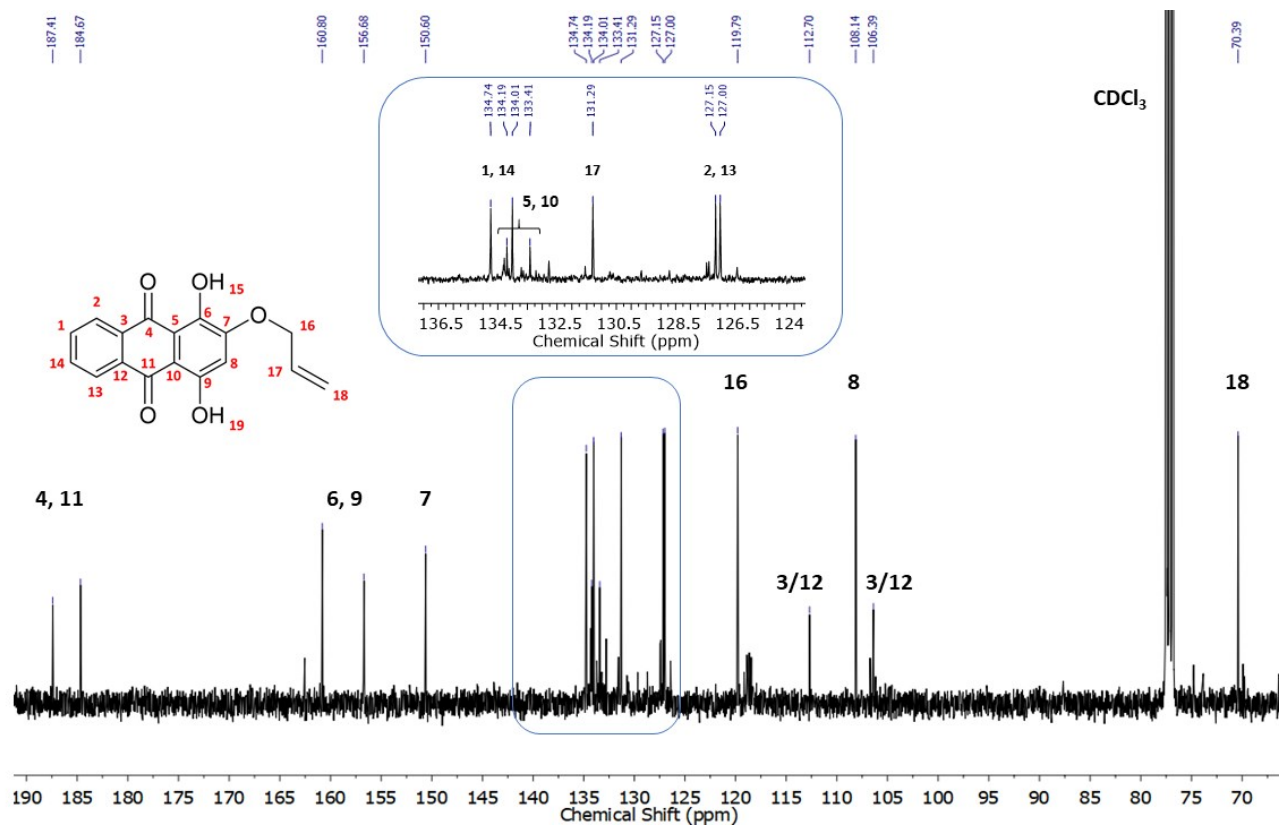


Figure S5. ^{13}C NMR spectrum of PmA in CDCl_3

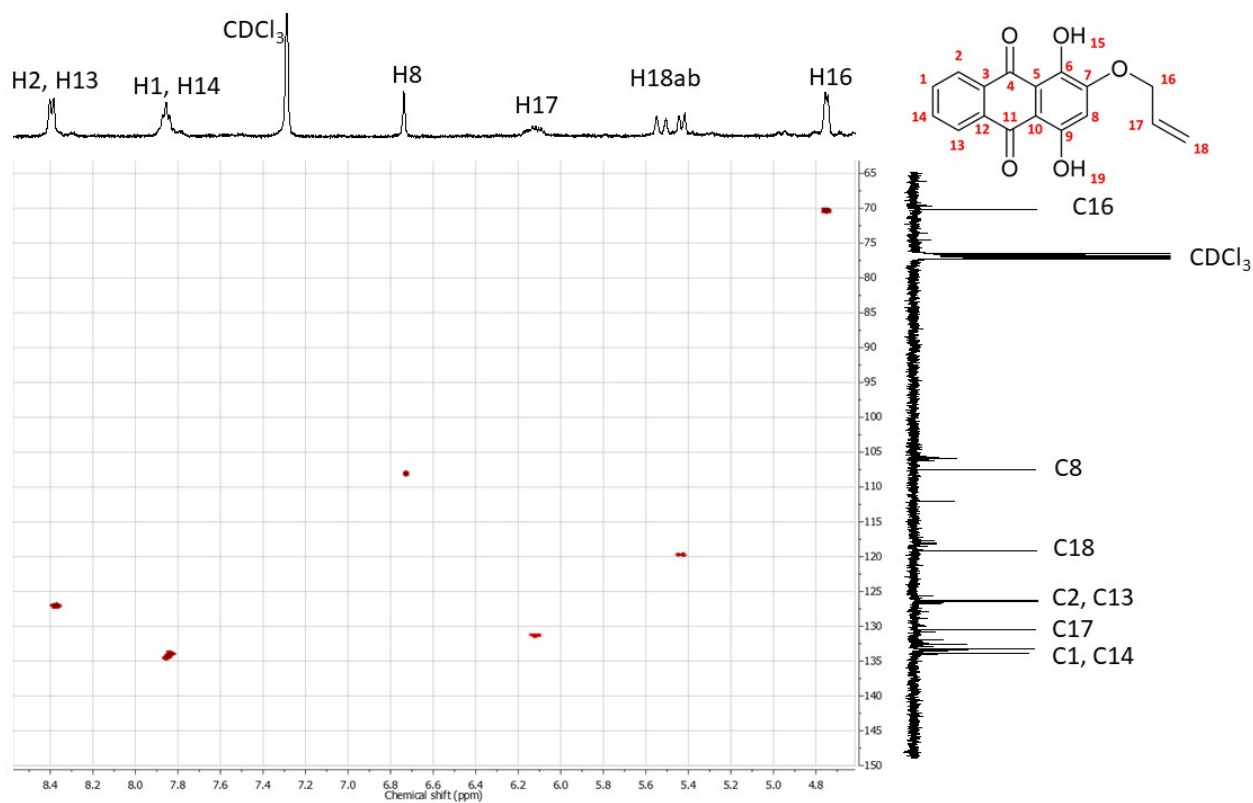


Figure S6. HSQC NMR spectrum of **PmA** in CDCl_3

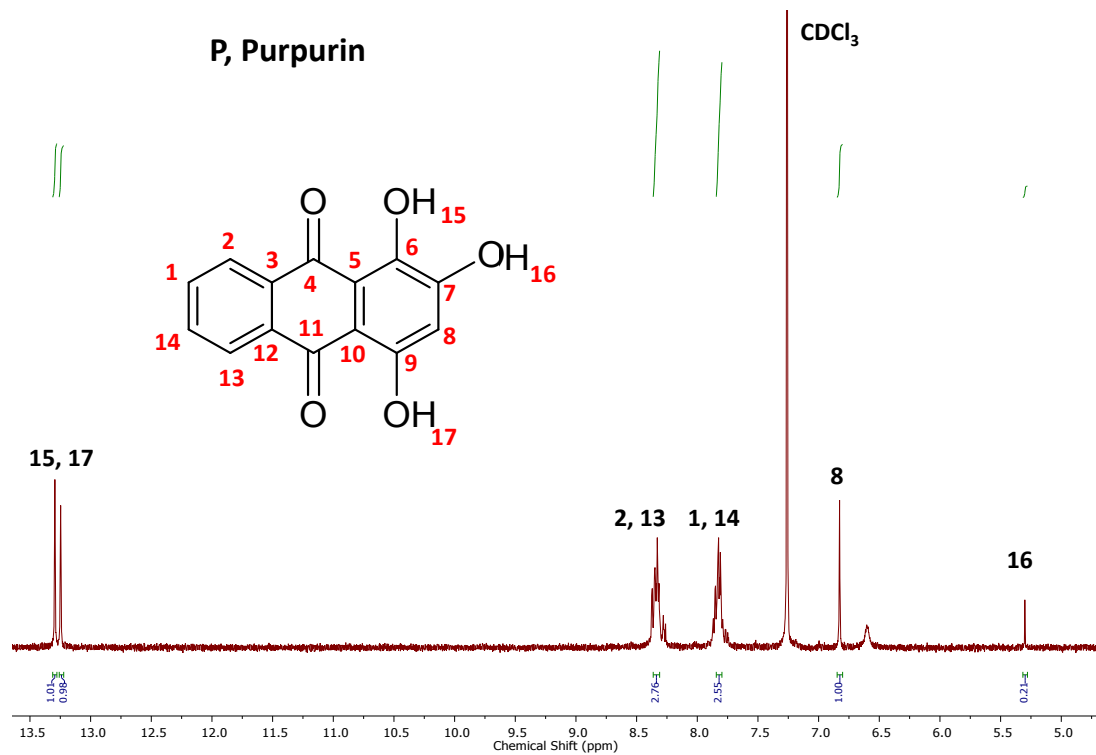


Figure S7. ^1H NMR spectrum of purpurin (**P**) in CDCl_3

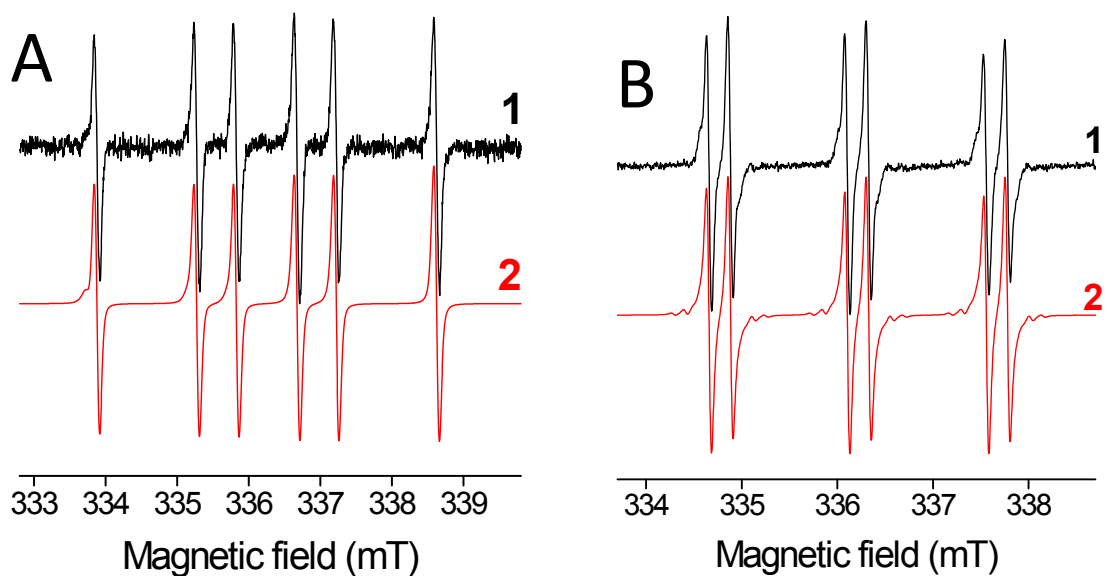


Figure S8. The normalized experimental (1) and simulated (2) EPR spectra obtained upon *in situ* LED@450 nm exposure of **P**/Iod/benzene solution in the presence of spin trapping agent under argon. **(A)** DMPO, exposure 225 s; EPR spectrometer settings: microwave frequency, ~ 9.44 GHz; microwave power, 11.35 mW; center field, ~ 336.3 mT; sweep width, 7 mT; gain, 1.00×10^5 ; modulation amplitude, 0.05 mT; sweep time, 45 s; time constant, 10.24 ms; number of scans, 5. **(B)** PBN, exposure 900 s; EPR spectrometer settings: microwave frequency, ~ 9.44 GHz; microwave power, 1.13 mW; center field, ~ 336.2 mT; sweep width, 5 mT; gain, 1.00×10^5 ; modulation amplitude, 0.025 mT; sweep time, 45 s; time constant, 10.24 ms; number of scans, 10.

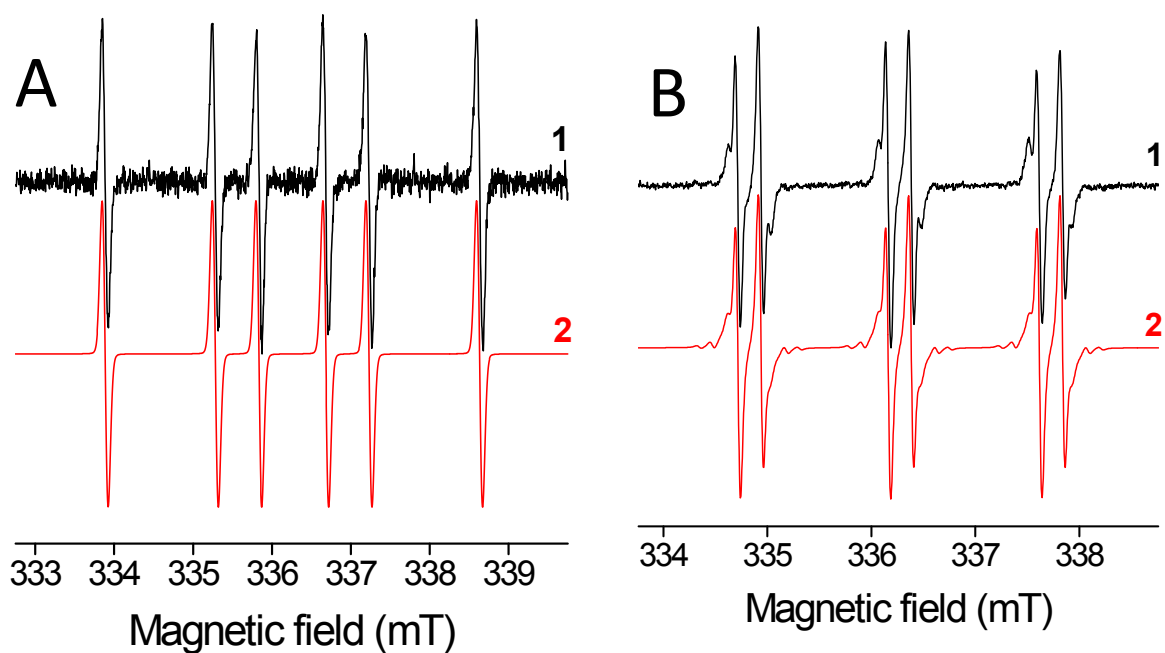


Figure S9. The normalized experimental (1) and simulated (2) EPR spectra obtained upon *in situ* LED@450 nm exposure of **PmA**/Iod/benzene solution in the presence of spin trapping agent under argon. **(A)** DMPO, exposure 450 s; EPR spectrometer settings: microwave frequency, ~ 9.44 GHz; microwave power, 1.12 mW; center field, ~ 336.2 mT; sweep width, 7 mT; gain, 1.00×10^5 ; modulation amplitude, 0.025 mT; sweep time, 45 s; time constant, 10.24 ms; number of scans, 5. **(B)** PBN, exposure 900 s; EPR spectrometer settings: microwave frequency, ~ 9.44 GHz; microwave power, 1.14 mW; center field, ~ 336.2 mT; sweep width, 5 mT; gain, 1.00×10^5 ; modulation amplitude, 0.025 mT; sweep time, 45 s; time constant, 10.24 ms; number of scans, 10.

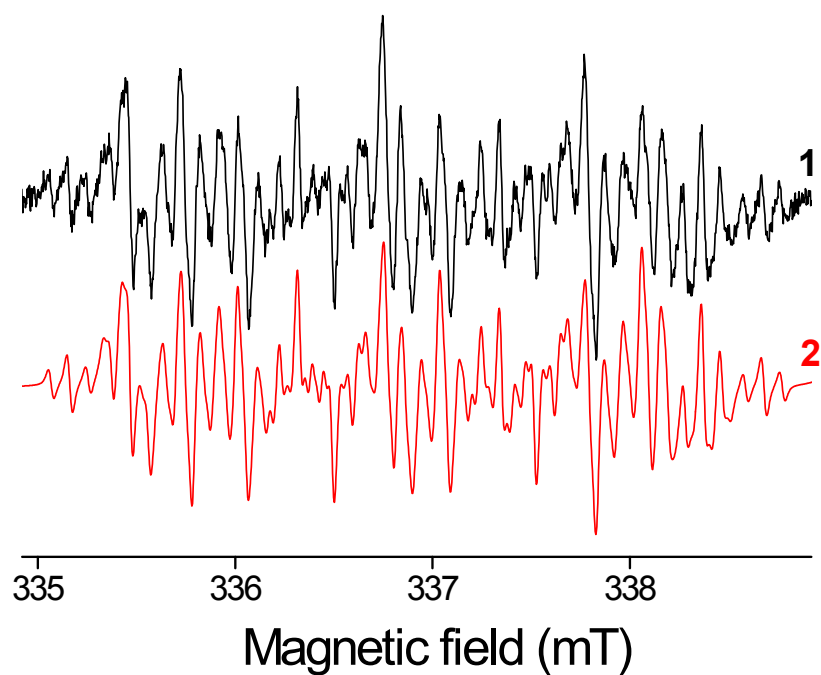


Figure S10. The normalized experimental (1) and simulated (2) EPR spectra obtained after 900 s *in situ* LED@450 nm exposure of **PmA**/Iod/benzene solution in the presence of ND spin trap under argon. EPR spectrometer settings: microwave frequency, ~ 9.44 GHz; microwave power, 1.15 mW; center field, ~336.4 mT; sweep width, 4 mT; gain, 1.00×10^5 ; modulation amplitude, 0.02 mT; sweep time, 90 s; time constant, 20.48 ms; number of scans, 10.

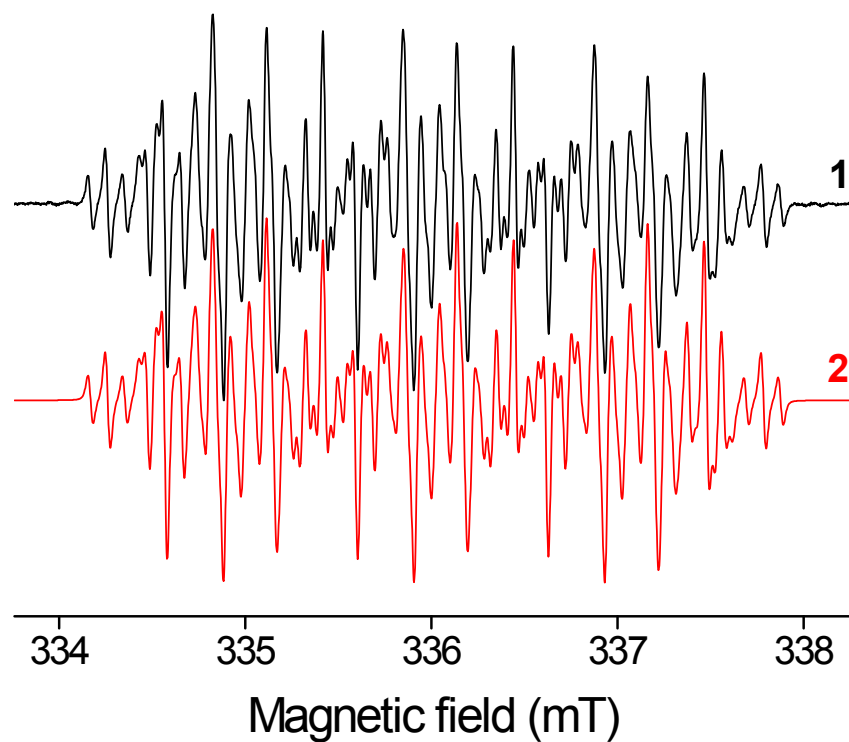


Figure S11. The normalized experimental (1) and simulated (2) EPR spectra obtained after 900 s *in situ* LED@400 nm exposure of PA/Iod/benzene solution in the presence of ND spin trap under argon. EPR spectrometer settings: microwave frequency, ~ 9.43 GHz; microwave power, 0.11 mW; center field, ~336.2 mT; sweep width, 4.5 mT; gain, 5.02×10^4 ; modulation amplitude, 0.01 mT; sweep time, 125 s; time constant, 20.48 ms; number of scans, 5.

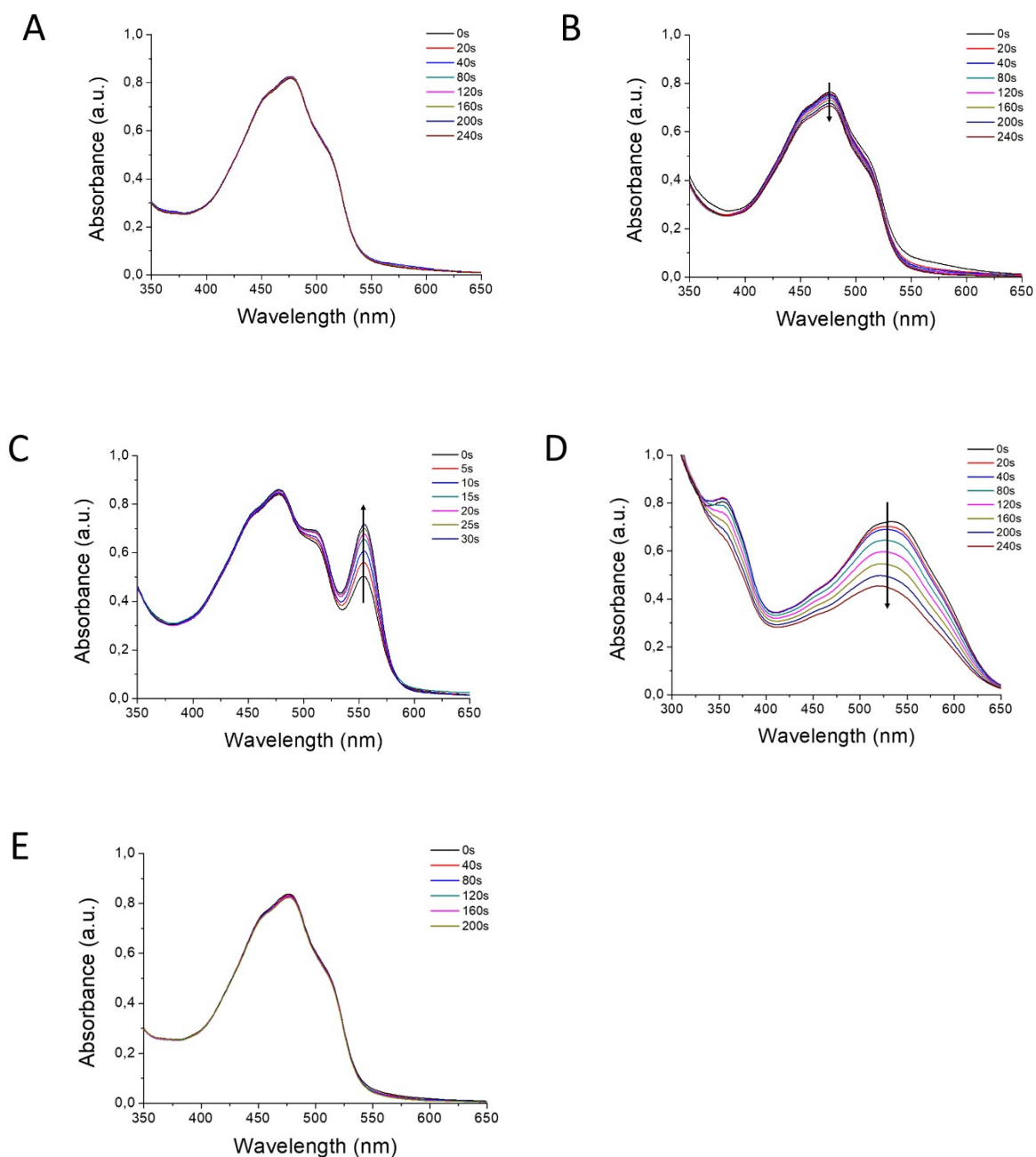


Figure S12. Steady-state photolysis of A) P, B) P/Iod, C) P/Iod/rhodamine B, D) P/MDEA and E) P/TT in ACN after irradiation by LED@405 nm (60 mW/cm²) under air conditions. [P] = 0.14 mM, [Iod] = 13 mM, [MDEA] = 30 mM, [Trithiol] = 10 mM, and [RhB] = 3.10⁻⁶ M.

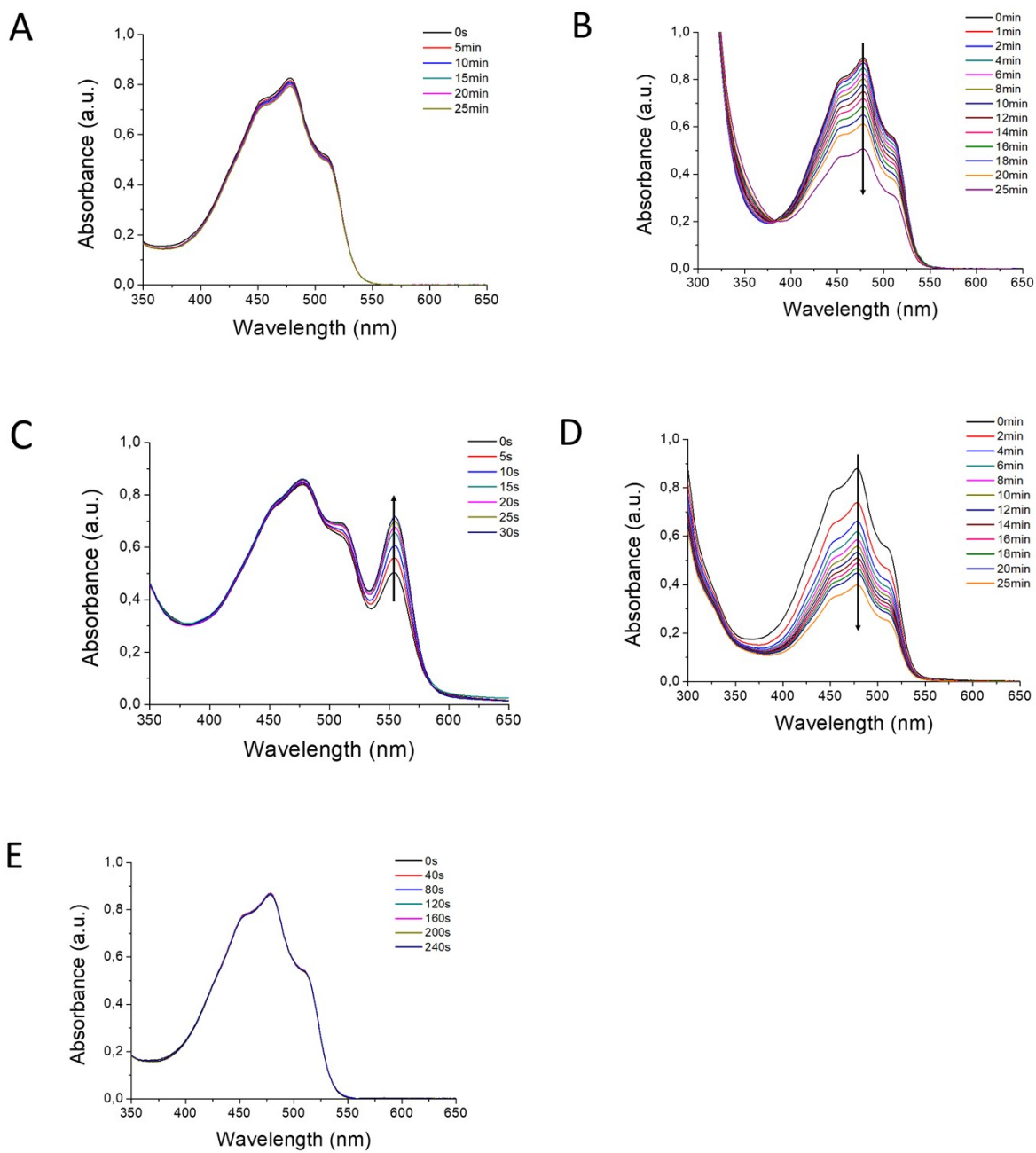


Figure S13. Steady-state photolysis of A) **PmA**, B) **PmA/Iod**, C) **PmA/Iod/ rhodamine B**, D) **PmA/MDEA** and E) **PmA/TT** in ACN after irradiation by LED@405 nm (60 mW/cm^2) under air conditions. $[\text{PmA}] = 0.12 \text{ mM}$, $[\text{Iod}] = 13 \text{ mM}$, $[\text{MDEA}] = 30 \text{ mM}$, $[\text{Trithiol}] = 10 \text{ mM}$, and $[\text{RhB}] = 3.10^{-6} \text{ M}$.

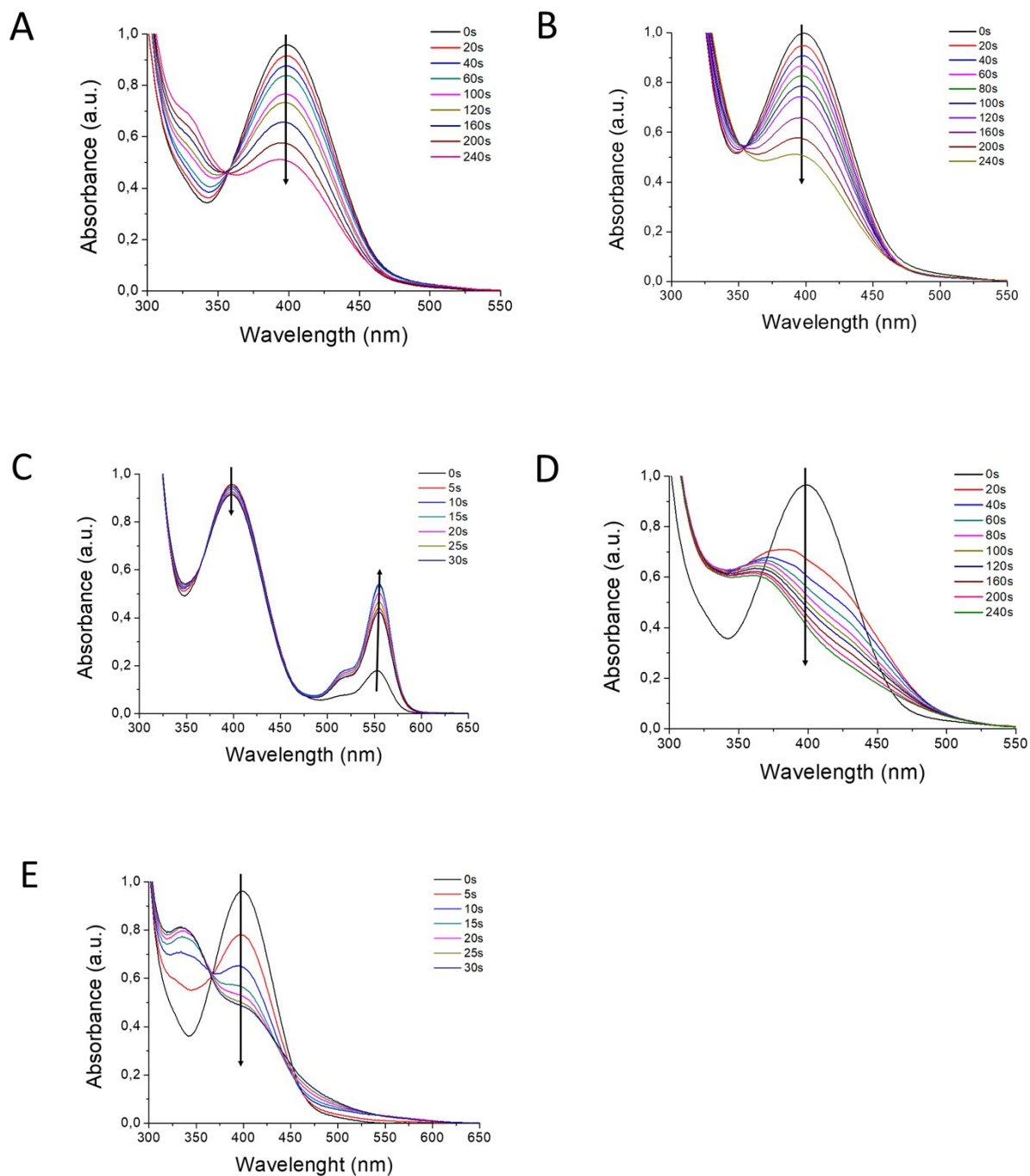
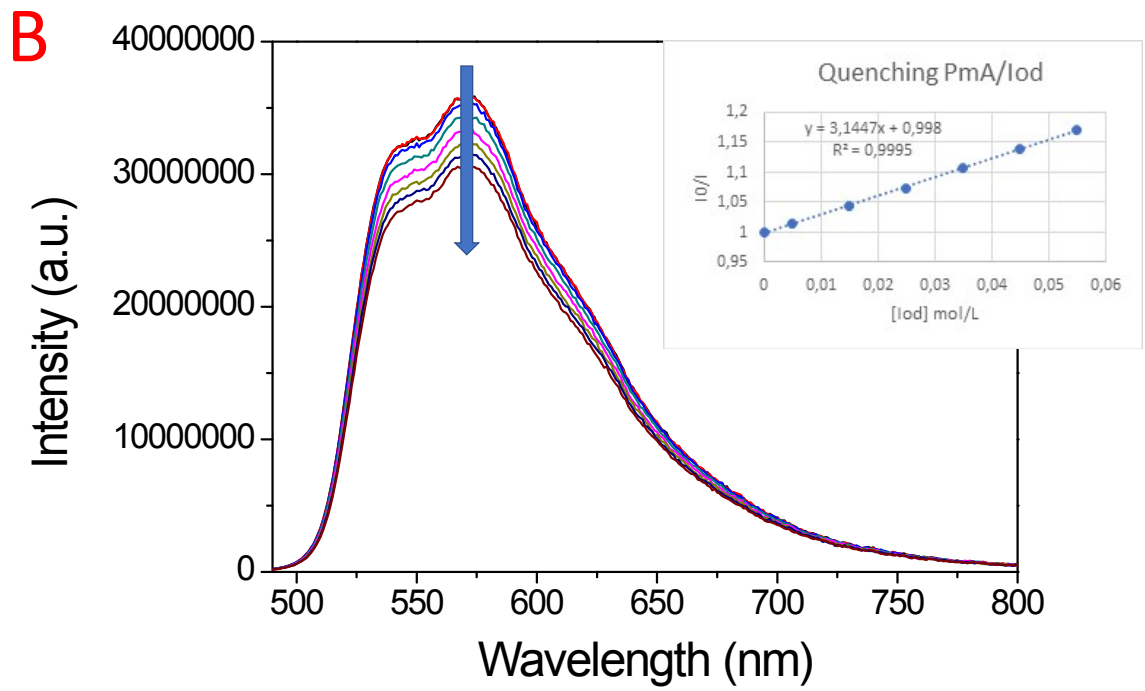
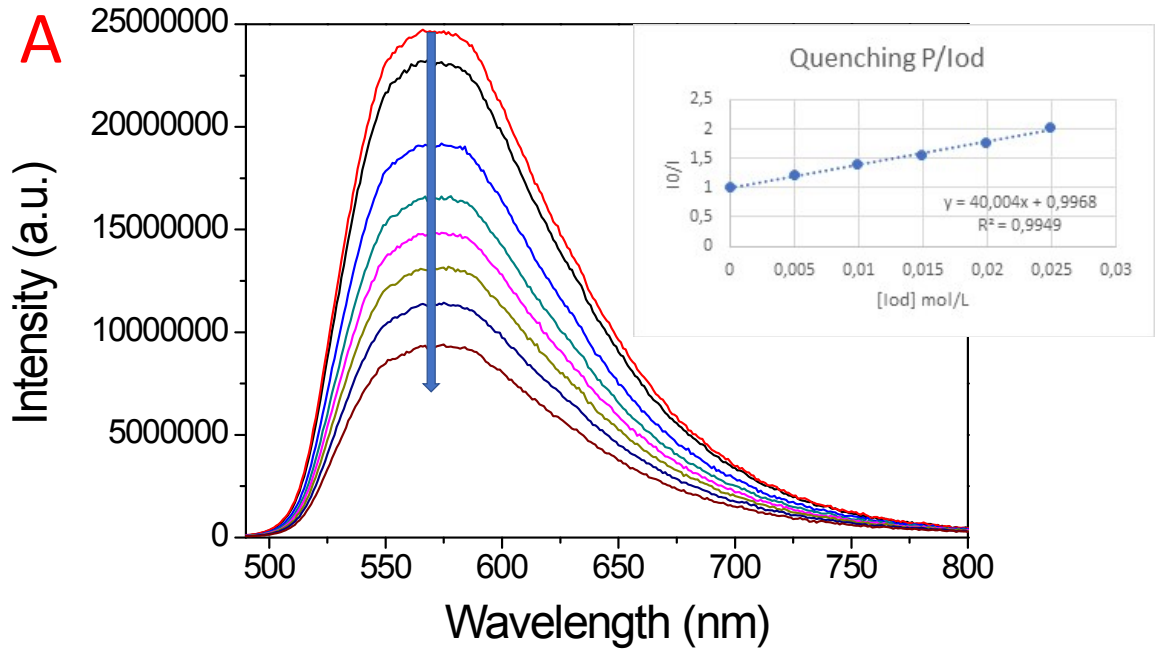


Figure S14. Steady-state photolysis of A) PA, B) PA/Iod, C) PA/Iod/ rhodamine B, D) PA/MDEA and E) PA/TT in ACN after irradiation by LED@405 nm (60 mW/cm^2) under air conditions. $[\text{PA}] = 0.10 \text{ mM}$, $[\text{Iod}] = 13 \text{ mM}$, $[\text{MDEA}] = 30 \text{ mM}$, $[\text{Trithiol}] = 10 \text{ mM}$, and $[\text{RhB}] = 3.10^{-6} \text{ M}$.



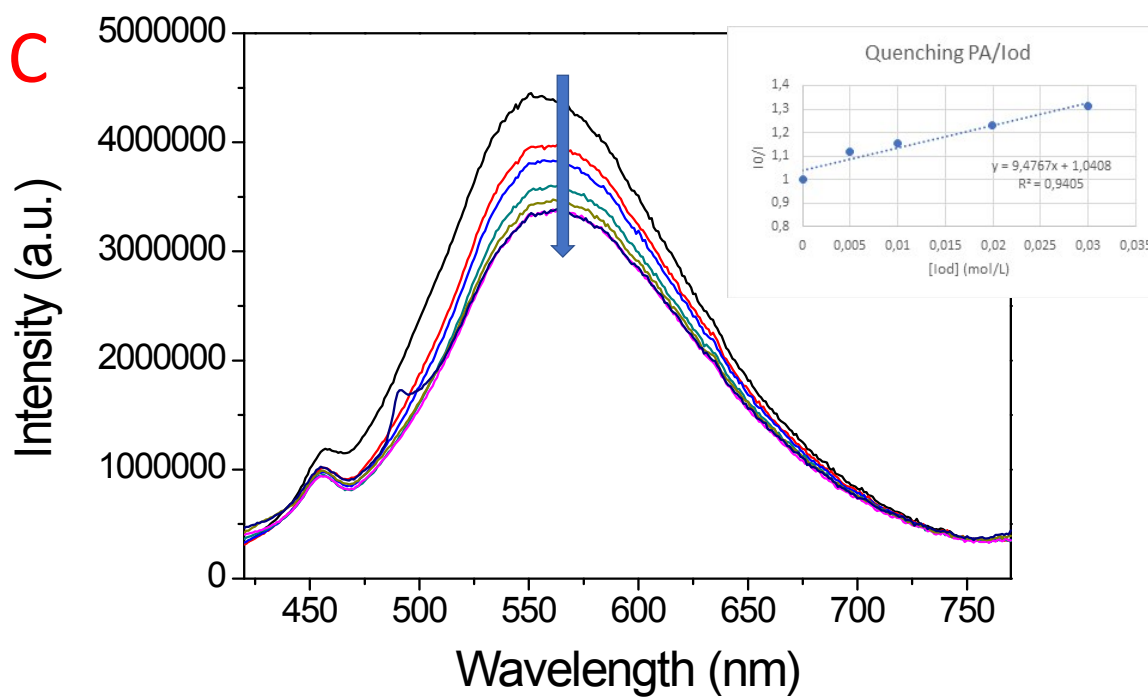


Figure S15. Fluorescence quenching of A) **P**, B) **PmA** and C) **PA** upon gradual addition of Iod in ACN. **Insert:** Stern-Volmer plot I_0/I as a function of the concentration of Iod for the calculation of the fluorescence quenching constants K_{SV} .

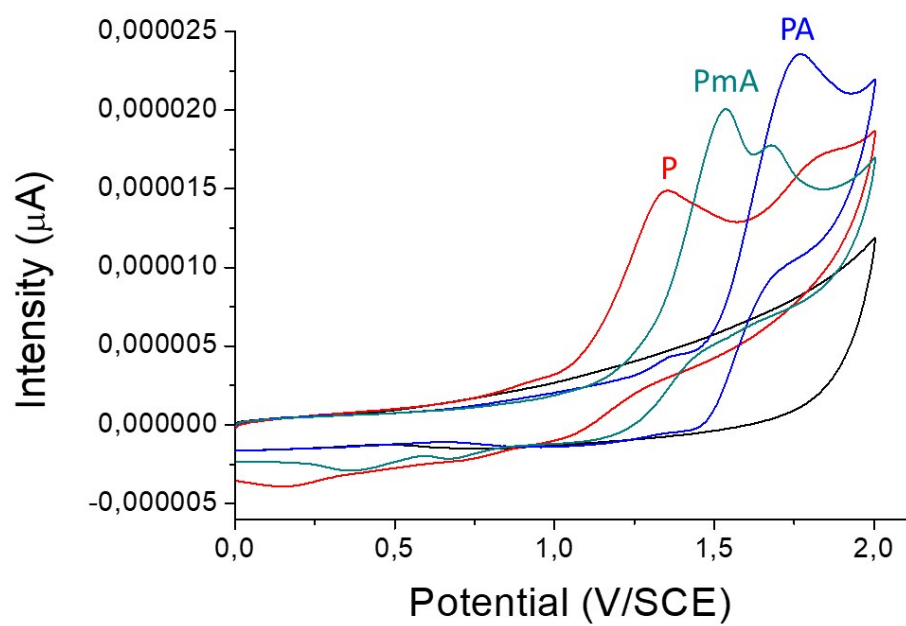
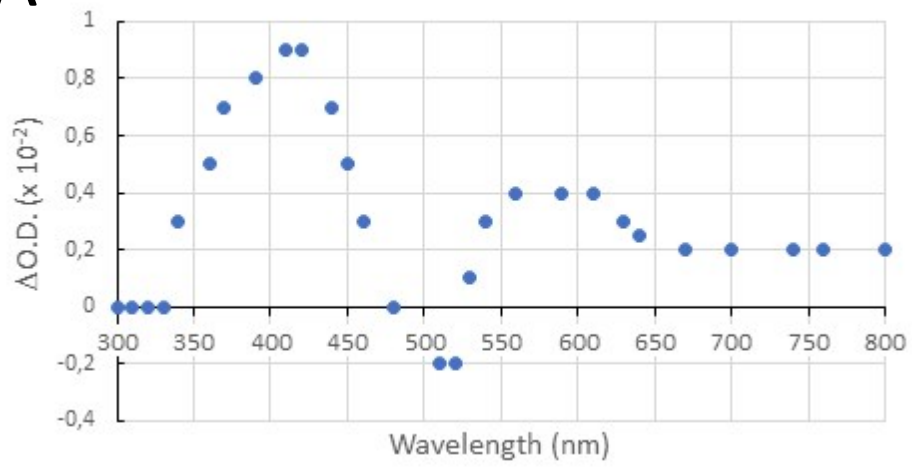
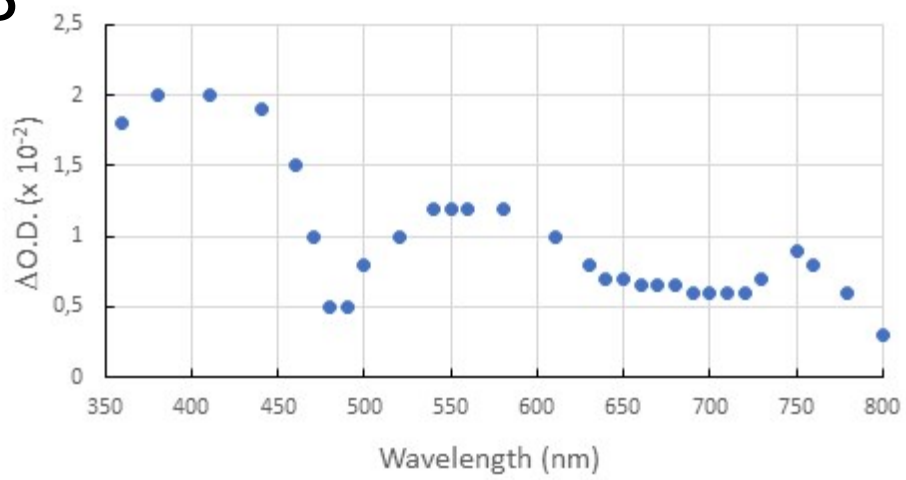


Figure S16. Cyclic voltammogram of purpurin (P), monoallyl purpurin (**PmA**) and triallyl purpurin (**PA**) in ACN + 10^{-3} M $n\text{Bu}_4\text{NBF}_4$ measured at a scan rate of 100 mV/s. $[\text{P}] = [\text{PmA}] = [\text{PA}] = 10^{-3}$ M.

A**Purpurin (P)****B****MonoAllyl-purpurin (PmA)**

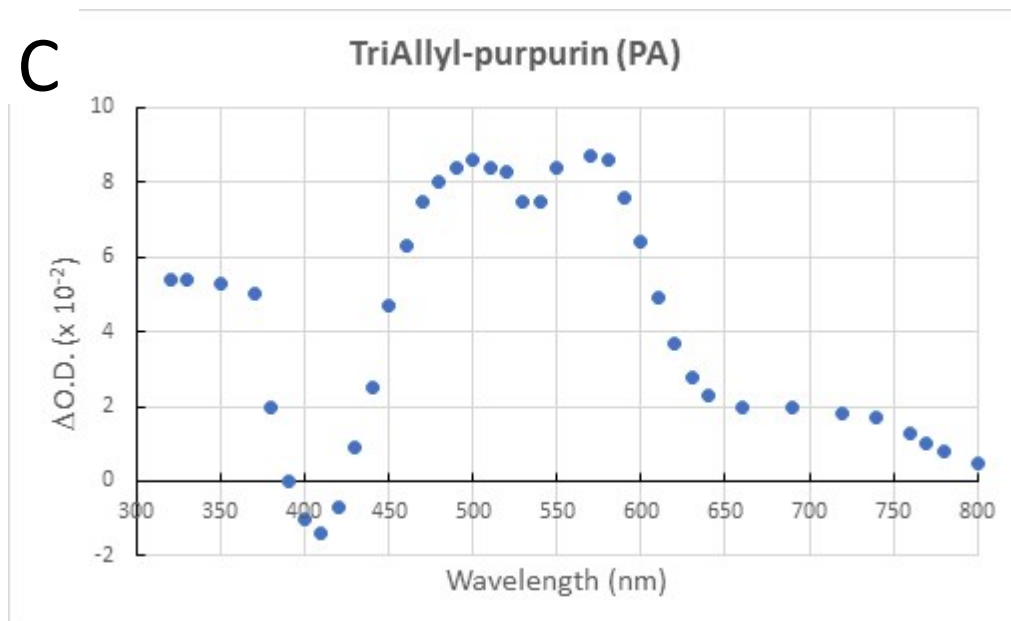
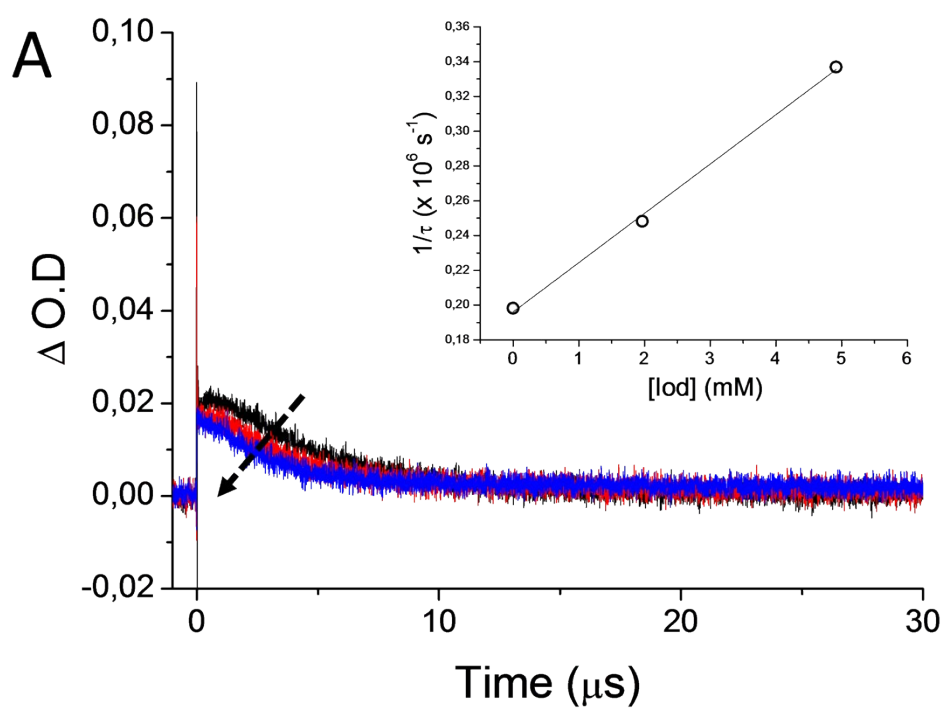


Figure S17. Transition absorption spectra of A) **P**, B) **PmA** and C) **PA** in ACN under argon atmosphere ($\lambda_{\text{ex}} = 355$ nm).



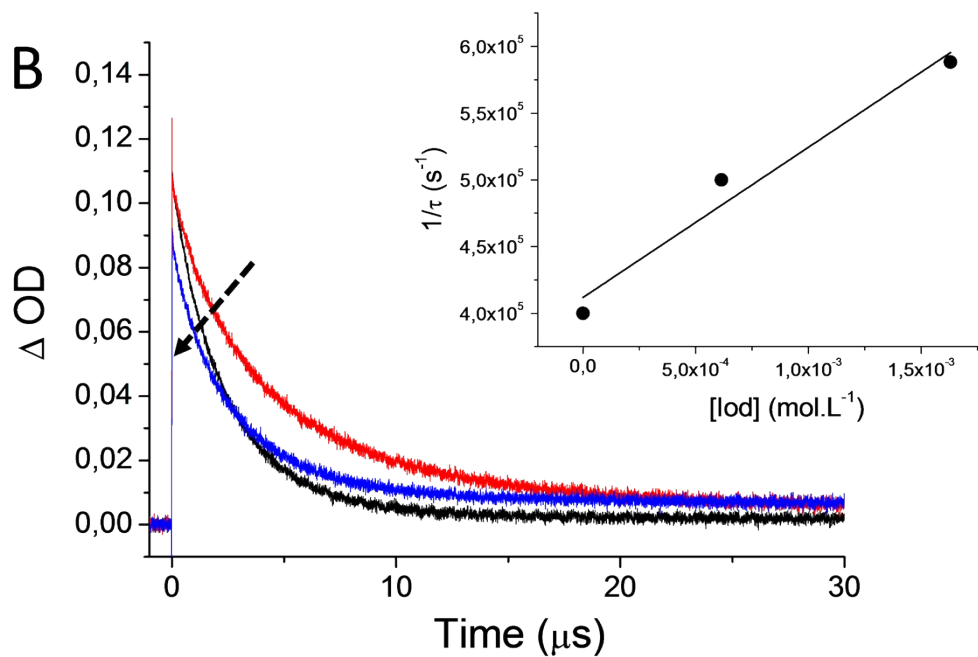


Figure S18. Decay traces of A) **PmA**/Iod at 410 nm and B) **PA**/Iod at 560 nm in ACN under argon atmosphere ($\lambda_{ex} = 355$ nm). **Insert:** Determination of the bimolecular quenching rate constants of A) $k_q^{Iod}(^3PmA^*)$ and B) $k_q^{Iod}(^3PA^*)$ using LFP ($\lambda_{ex} = 355$ nm, 7 ns pulse width). Pseudo-first-order decay rate constant of $^3PA^*$ monitored at 560 nm vs. varying concentration of Iod.

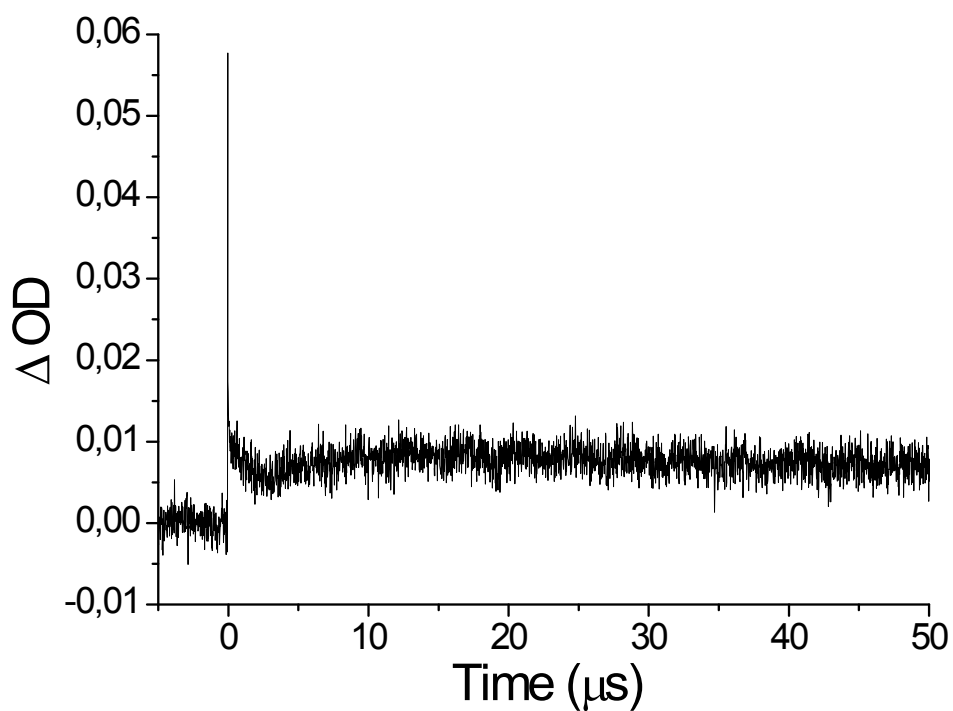


Figure S19. Decay traces of PA/Iod at 700 nm in ACN under argon atmosphere ($\lambda_{\text{ex}} = 355 \text{ nm}$).

Lifetime $> 150 \mu\text{s}$.

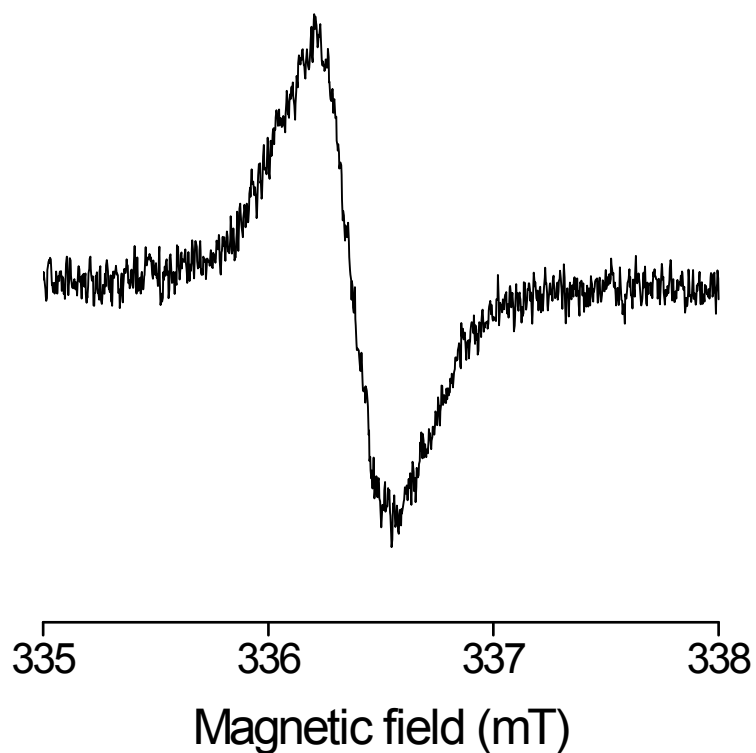


Figure S20. EPR spectrum measured upon 1350 s *in situ* LED@450 nm exposure of P/MDEA/benzene solution under argon. EPR spectrometer settings: microwave frequency, $\sim 9.44 \text{ GHz}$; microwave

power, 1.12 mW; center field, ~336.4 mT; sweep width, 3 mT; gain, 1.00×10^5 ; modulation amplitude, 0.05 mT; sweep time, 45 s; time constant, 20.48 ms; number of scans, 5.

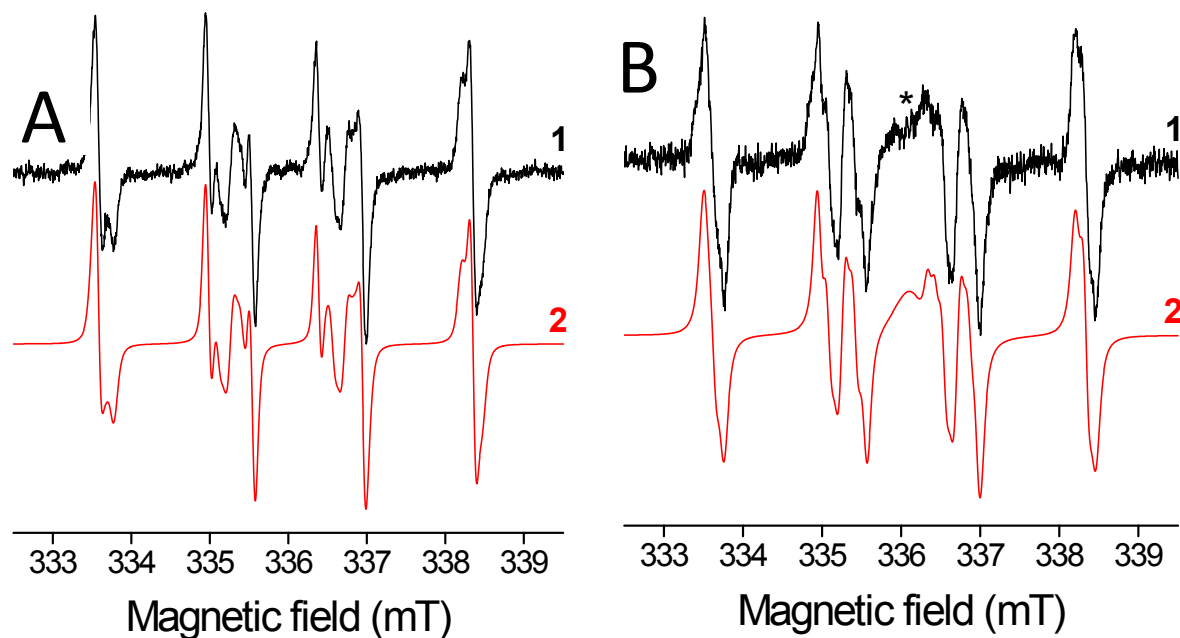


Figure S21. The normalized experimental (1) and simulated (2) EPR spectra obtained upon *in situ* LED@450 nm irradiation of P/MDEA/benzene solution in the presence of DMPO spin trap under argon (* denotes of purpurin anthrasemiquinone radical). (A) exposure 225 s ; (B) exposure 675 s. EPR spectrometer settings : microwave frequency, ~9.43 GHz ; microwave power, 10.93 mW; center field, ~336.0 mT; sweep width, 7 mT; gain, 1.00×10^5 ; modulation amplitude, 0.05 mT; sweep time, 45 s; time constant, 10.24 ms; number of scans, 5.

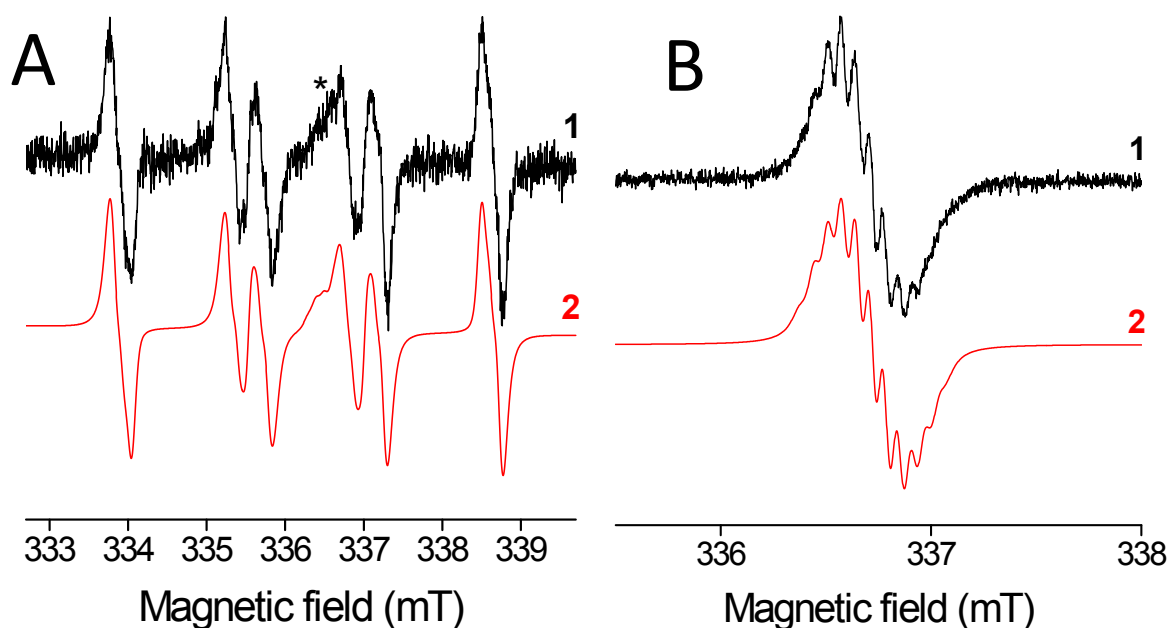


Figure S22. The normalized experimental (1) and simulated (2) EPR spectra obtained upon 900s *in situ* LED@450 nm exposure of benzene solutions under argon. (A) **PmA/MDEA/DMPO** (* denotes signal of **PmA** anthrasemiquinone radical); EPR spectrometer settings: microwave frequency, ~ 9.44 GHz; microwave power, 11.32 mW; center field, ~ 336.2 mT; sweep width, 7 mT; gain, 1.00×10^5 ; modulation amplitude, 0.05 mT; sweep time, 45 s; time constant, 10.24 ms; number of scans, 10 and (B) **PmA/MDEA**; EPR spectrometer settings: microwave frequency, ~ 9.44 GHz; microwave power, 1.15 mW; center field, ~ 336.7 mT; sweep width, 2 mT; gain, 1.00×10^5 ; modulation amplitude, 0.05 mT; sweep time, 45 s; time constant, 10.24 ms; number of scans, 10.

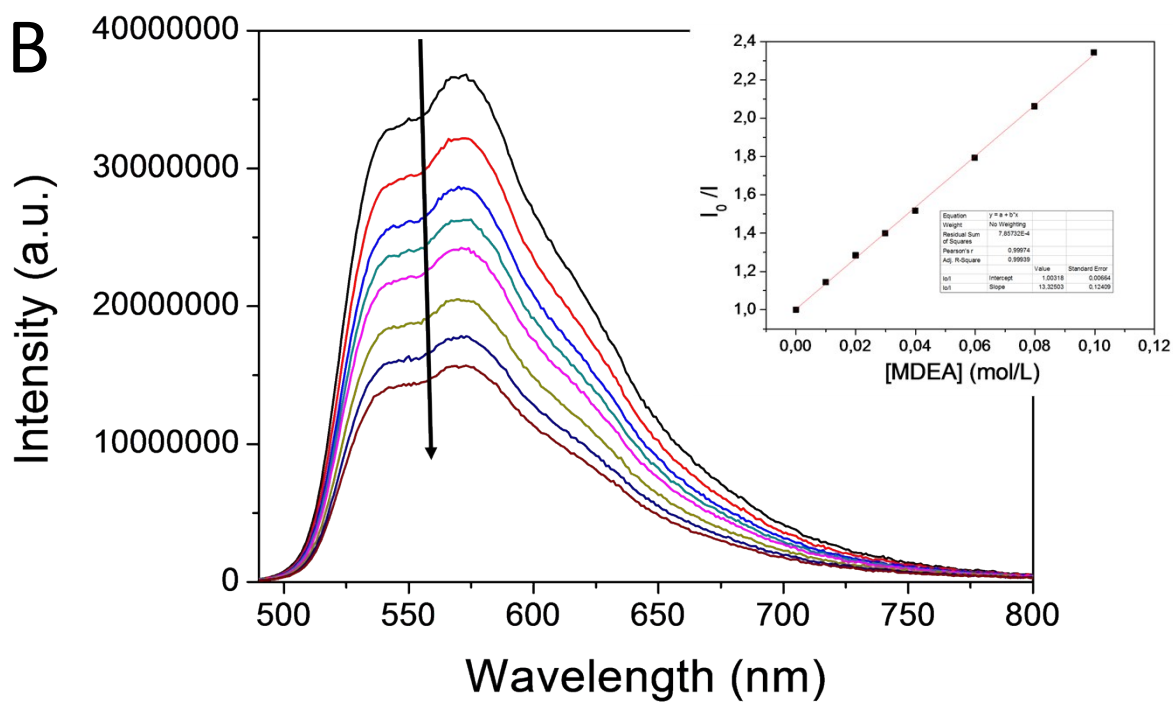
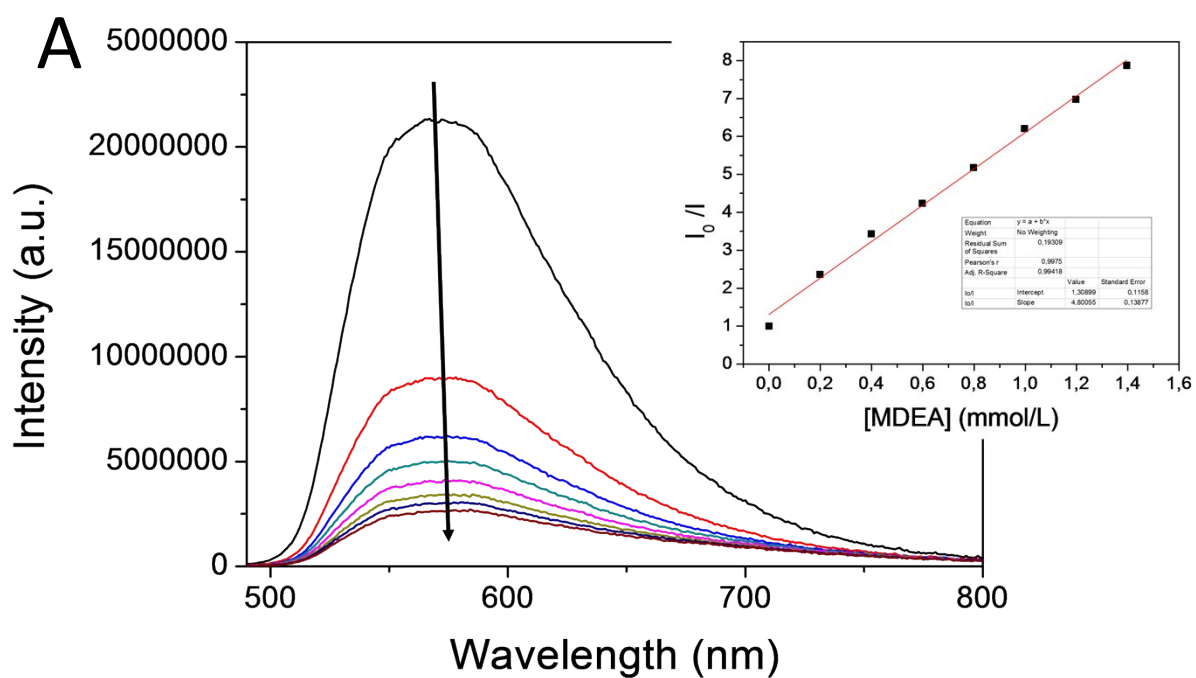


Figure S23. Fluorescence quenching of A) **P** and B) **PmA** upon gradual addition of MDEA in ACN ($\lambda_{exc} = 480$ nm). **Insert:** Stern-Volmer plot I_0/I as a function of the concentration of MDEA for the calculation of the fluorescence quenching constants K_{SV} .

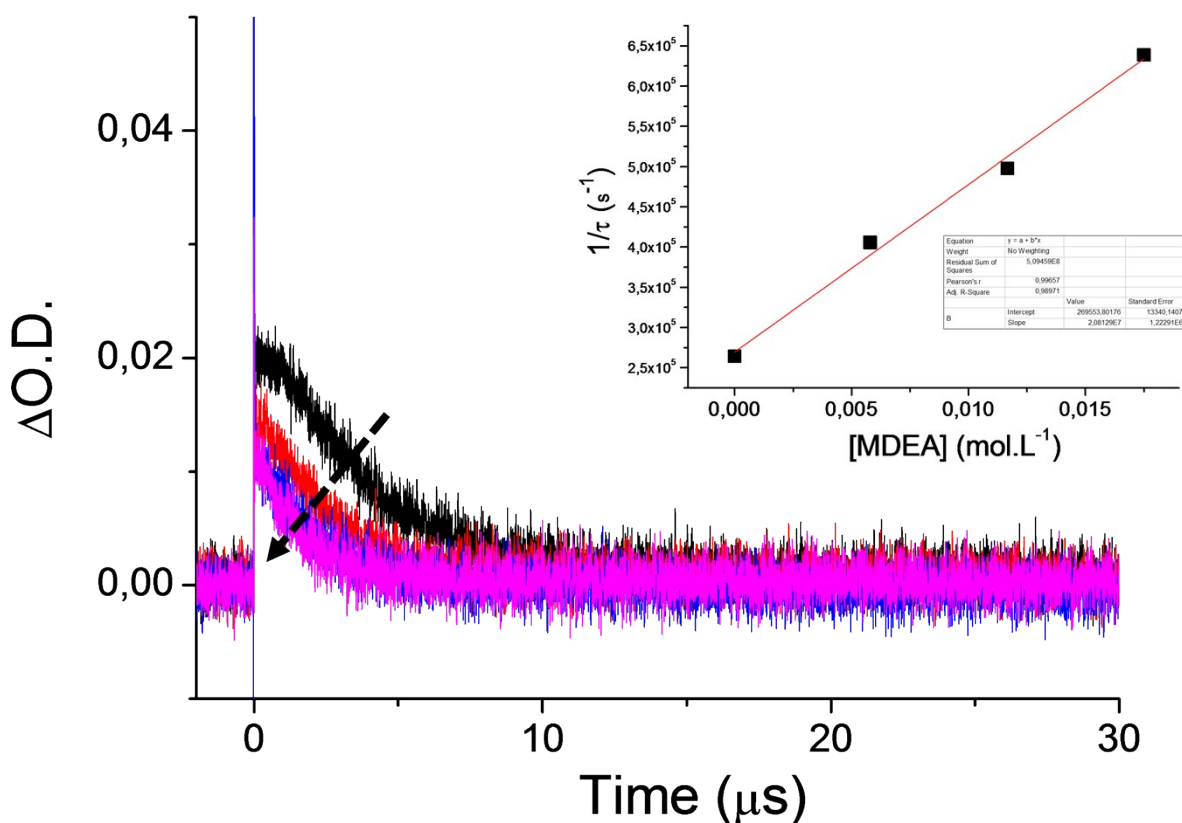


Figure S24. Decay traces of **PmA**/MDEA at 410 nm in ACN under argon atmosphere ($\lambda_{\text{ex}} = 355$ nm). **Insert:** Determination of the bimolecular quenching rate constants of $k_q^{\text{MDEA}}(^3\text{PmA}^*)$ using LFP ($\lambda_{\text{ex}} = 355$ nm, 7 ns pulse width). Pseudo-first-order decay rate constant of $^3\text{PmA}^*$ monitored at 410 nm vs. varying MDEA concentration.

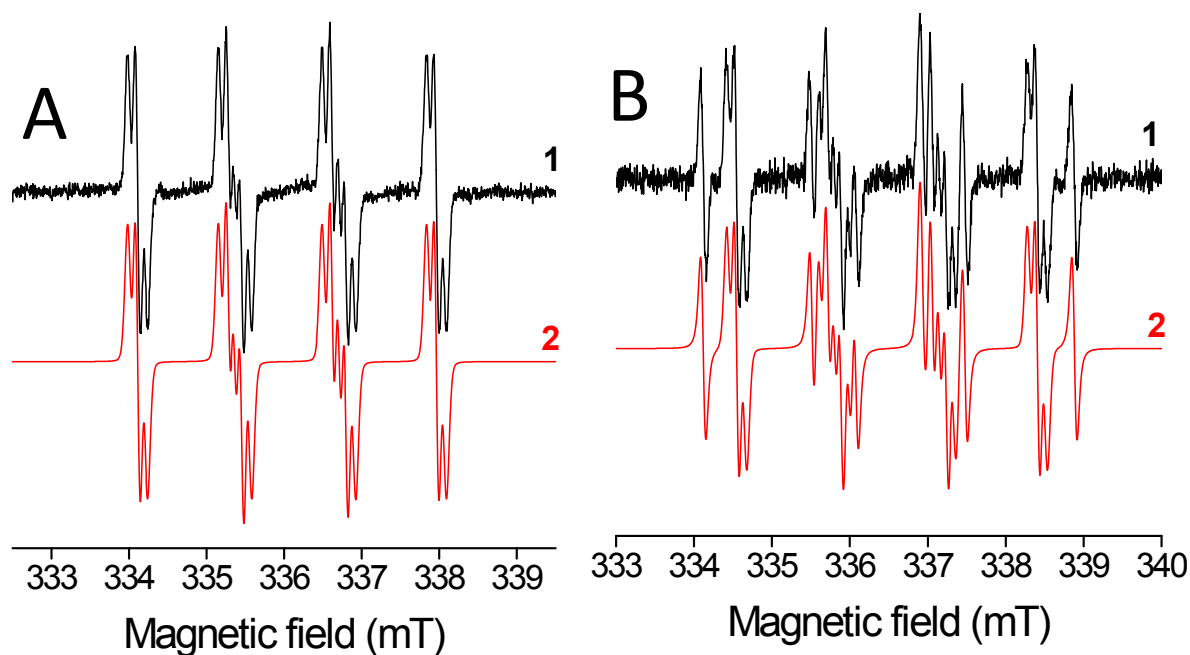


Figure S25. The normalized experimental (1) and simulated (2) EPR spectra obtained upon 450 s *in situ* LED@450 nm exposure of benzene solutions under argon: (A) P/TT/DMPO; (B) P/TT/Iod/DMPO. EPR spectrometer settings: microwave frequency, ~ 9.44 GHz; microwave power, 1.11 mW; center field, ~336.0 or ~336.5 mT; sweep width, 7 mT; gain, 1.00×10^5 ; modulation amplitude, 0.025 mT; sweep time, 45 s; time constant, 10.24 ms; number of scans, 10.

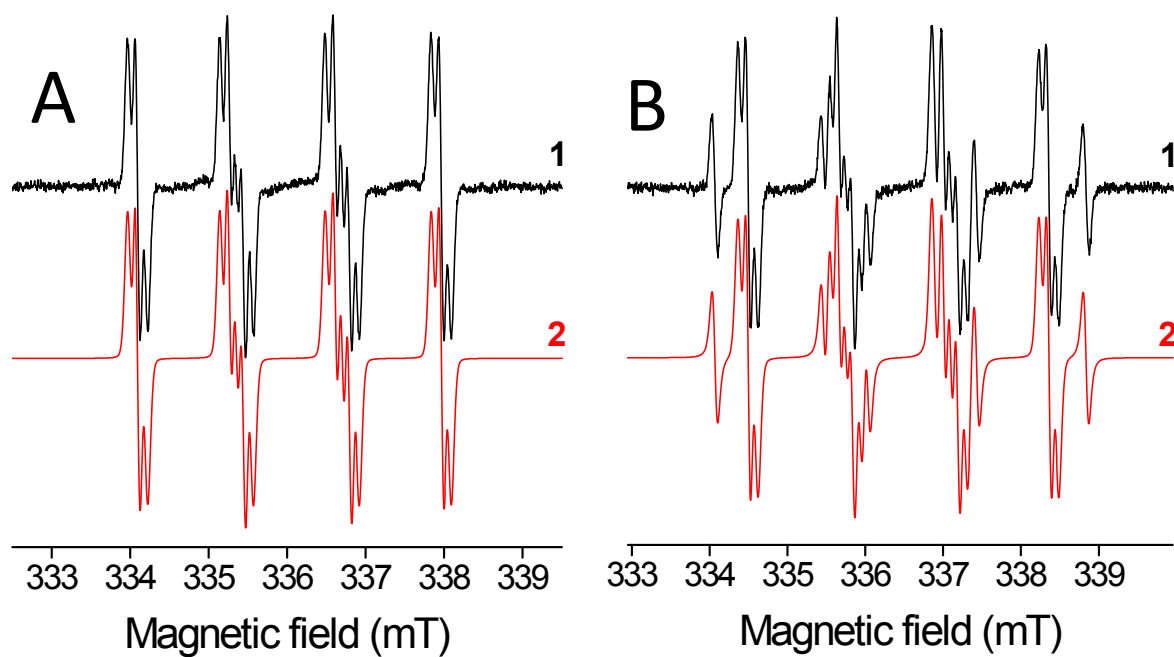


Figure S26. The normalized experimental (1) and simulated (2) EPR spectra obtained upon 450 s *in situ* LED@450 nm exposure of benzene solutions under argon: (A) **PmA/TT/DMPO**; (B) **PmA/TT/Iod/DMPO**. EPR spectrometer settings: microwave frequency, ~9.44 GHz; microwave power, 1.11 mW; center field, ~336.0 or ~336.5 mT; sweep width, 7 mT; gain, 1.00×10^5 ; modulation amplitude, 0.025 mT; sweep time, 45 s; time constant, 10.24 ms; number of scans, 10.

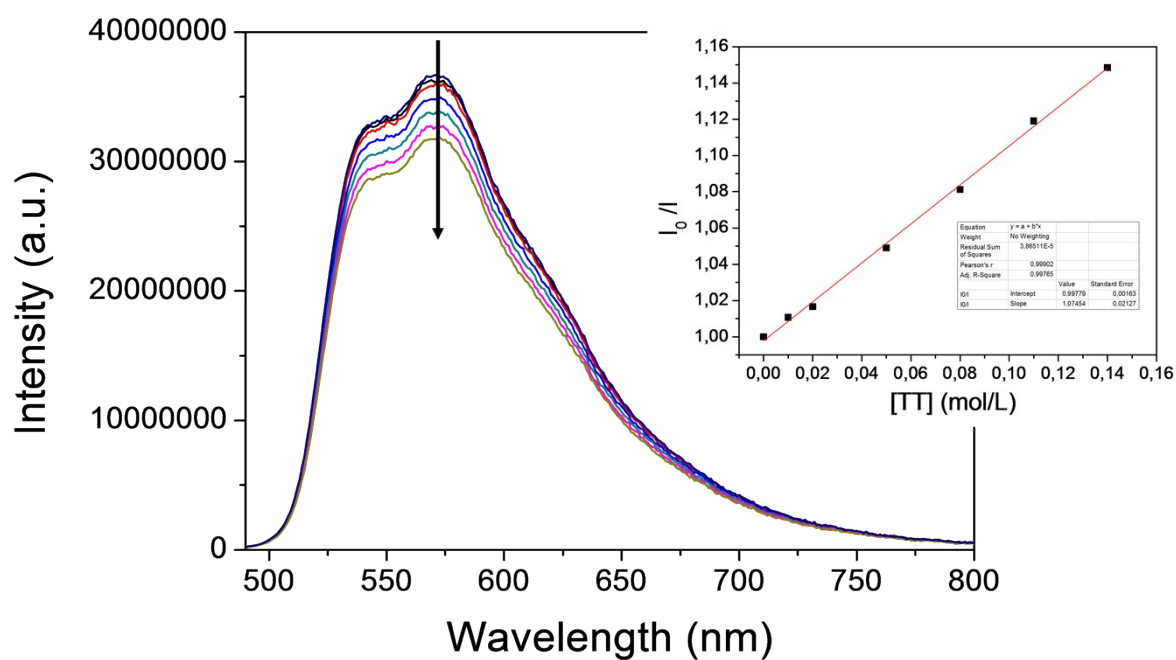


Figure S27. Fluorescence quenching of **PmA** upon gradual addition of **TT** in **ACN** ($\lambda_{\text{exc}} = 480$ nm). **Insert:** Stern-Volmer plot I_0/I as a function of the concentration of **TT** for the calculation of the fluorescence quenching constants K_{SV} .

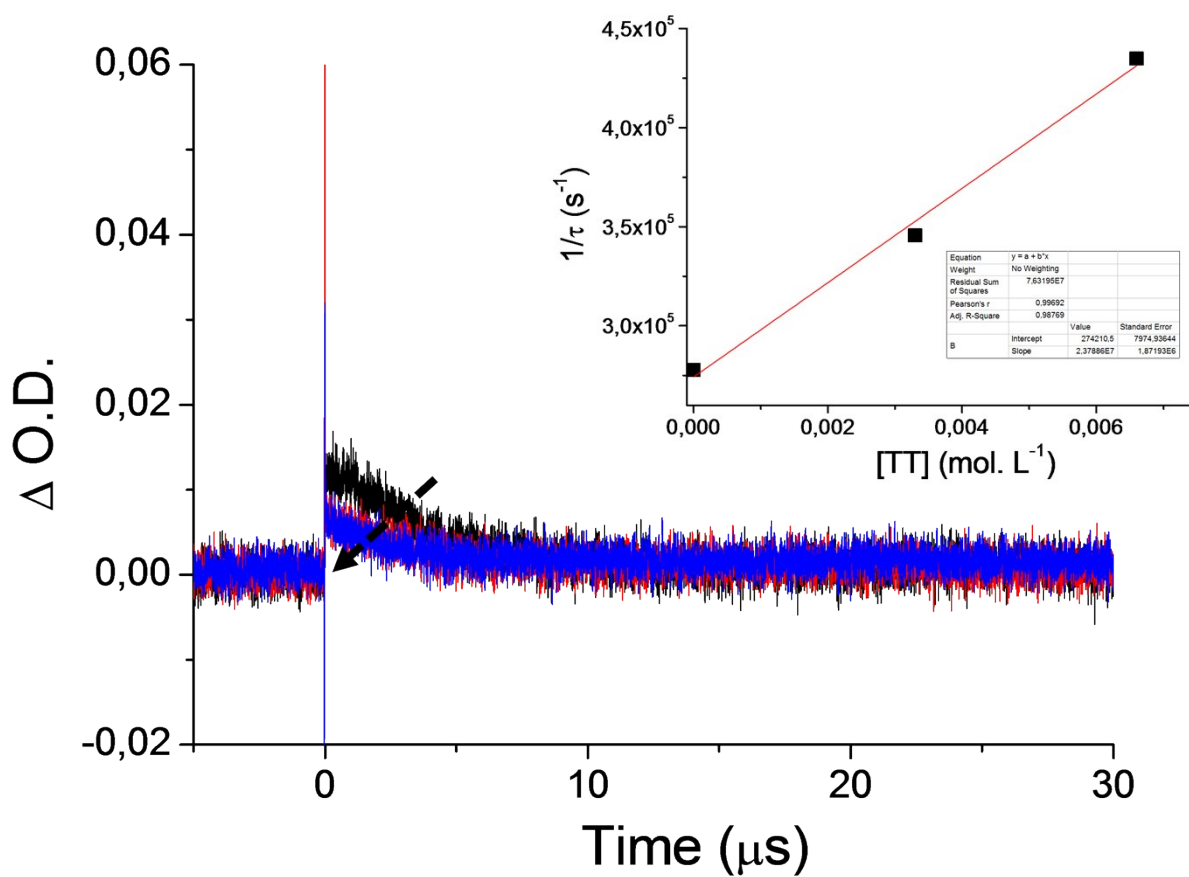


Figure S28. Decay traces of P/TT at 410 nm in ACN under argon atmosphere ($\lambda_{ex} = 355$ nm).

Insert: Determination of the bimolecular quenching rate constants of A) $k_q^{TT} (^3P^*)$ using LFP ($\lambda_{ex} = 355$ nm, 7 ns pulse width). Pseudo-first-order decay rate constant of $^3P^*$ monitored at 410 nm vs. varying concentration of TT.

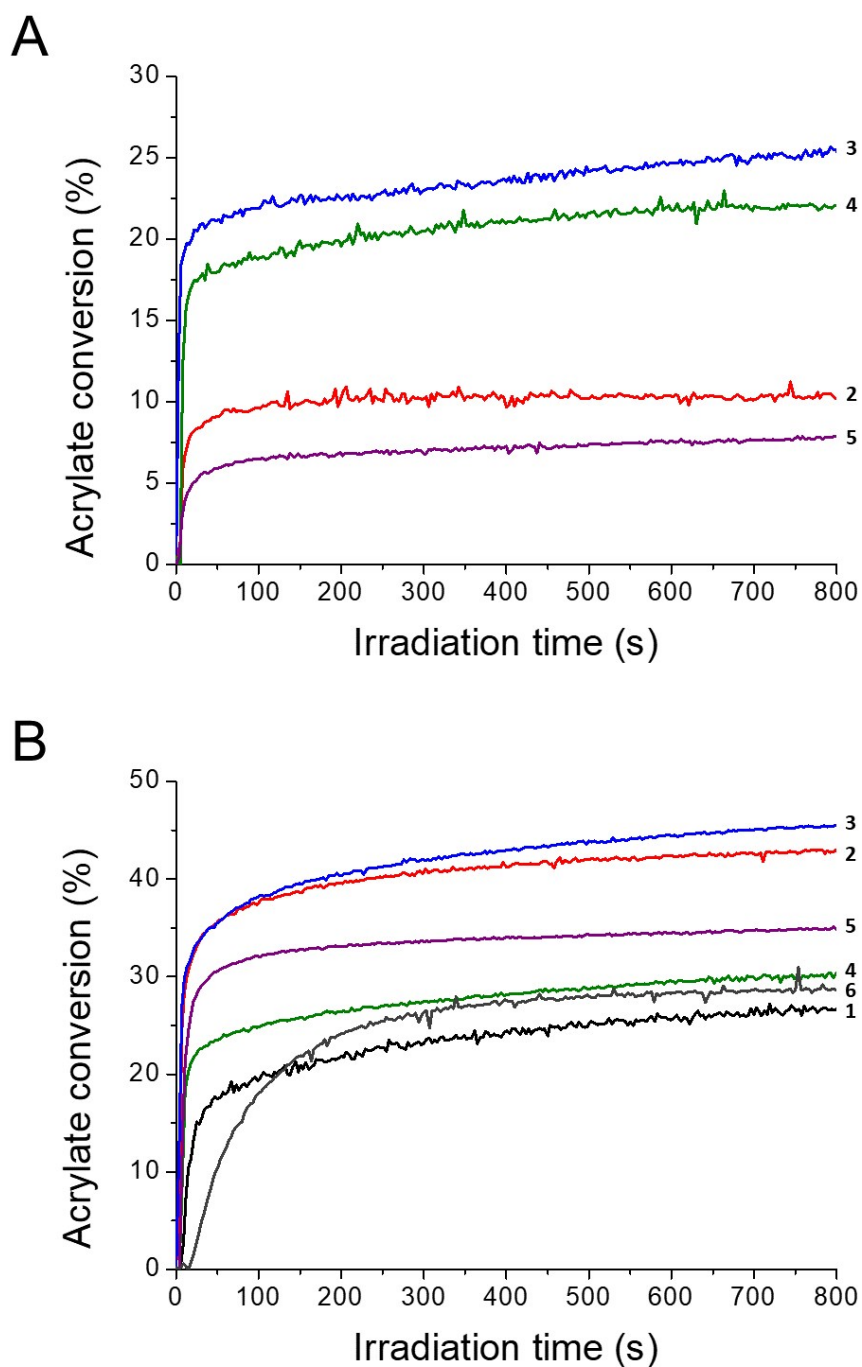


Figure S29. Kinetics profiles of TMPTA in the presence of **PmA**/MDEA (0.5/2%, w/w) (A) under air and B) in laminate conditions upon exposure (1) Xe lamp, (2) LED@385 nm, (3) LED@405nm, (4) LED@455 nm, (5) LED@470 nm and (6) LED@530 nm irradiation. Thickness of the film = 25 μm .

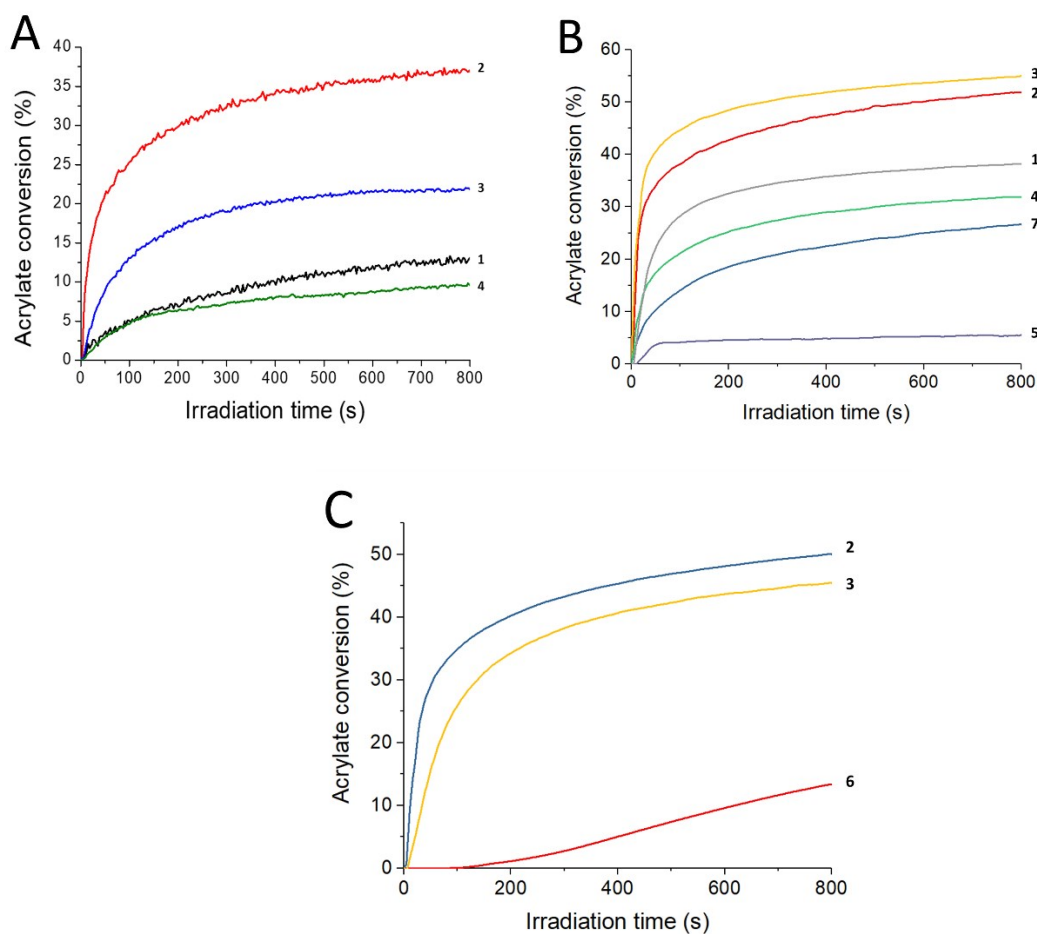
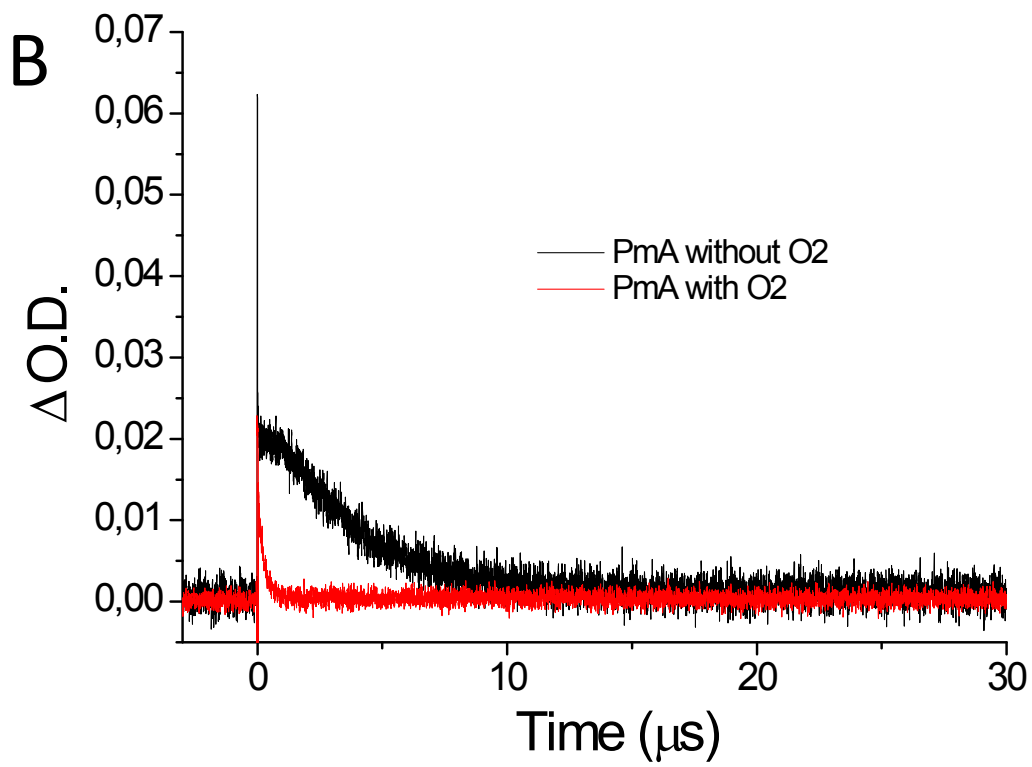
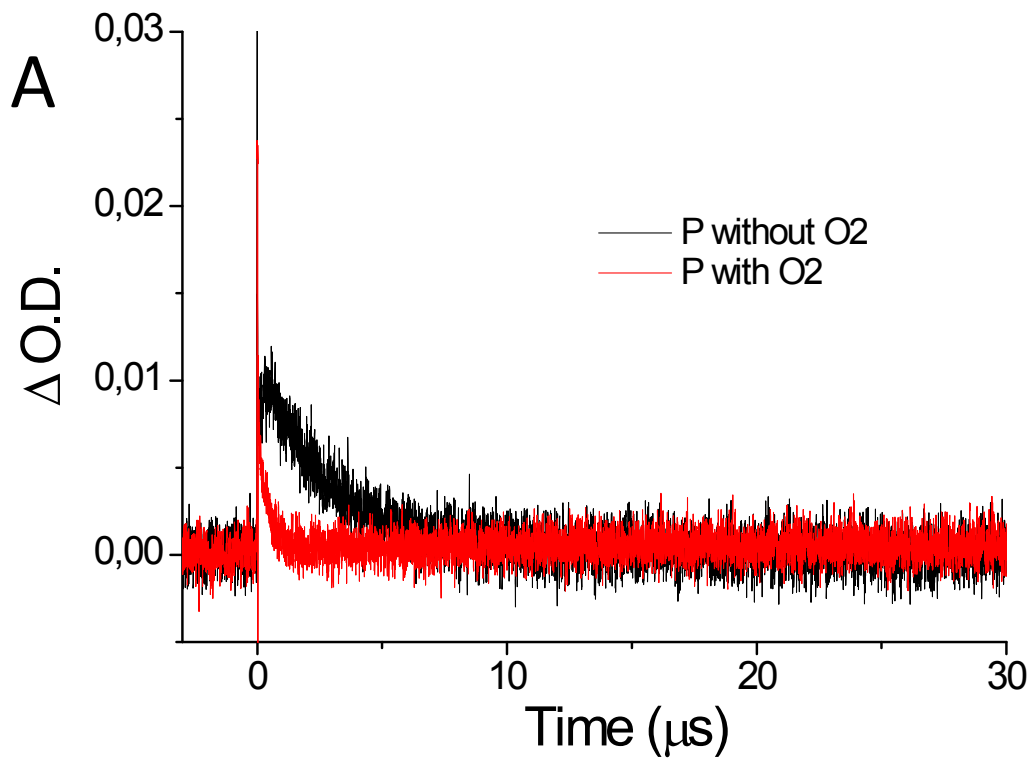


Figure S30. Kinetics profiles of TMPTA in the presence of (A) **P**/MDEA (0.5/2%, w/w), (B) **AQ**/MDEA (0.5/2%, w/w) and (C) **BP**/MDEA (0.5/2%, w/w): in laminate conditions upon exposure (1) Xe lamp, (2) LED@385 nm, (3) LED@405nm, (4) LED@455nm and (5) LED@470nm irradiation; and under air upon exposure (6) LED@385nm and (7) LED@405nm irradiation. Thickness of the film = 25 μm .



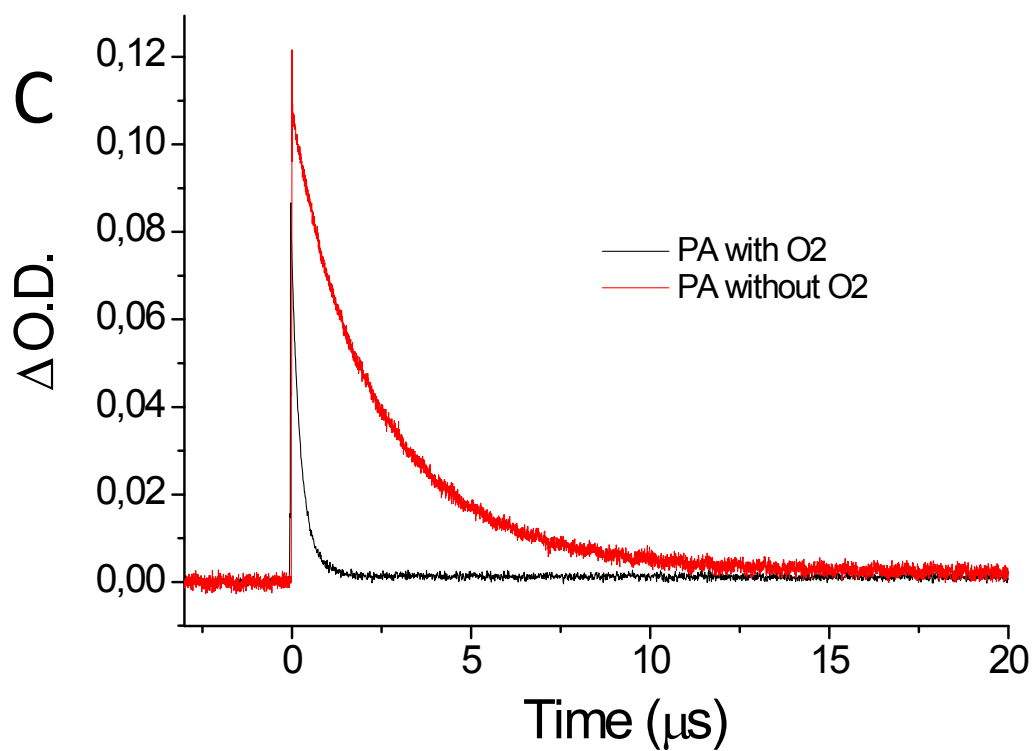


Figure S31. Decay traces of A) **P** (410 nm), B) **PmA** (410 nm) and C) **PA** (560 nm) in ACN with and without oxygen using LFP ($\lambda_{ex} = 355$ nm, 7 ns pulse width).

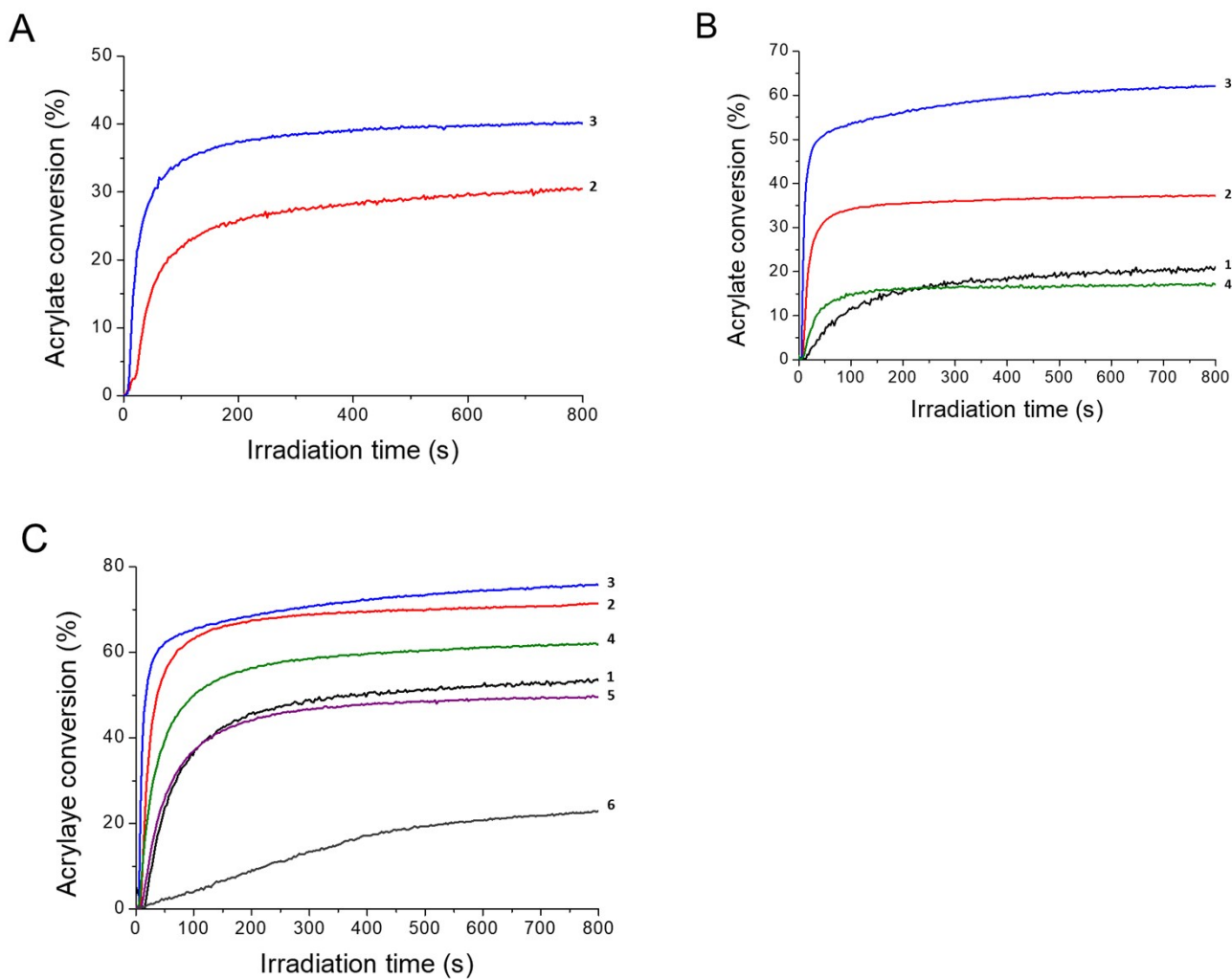


Figure S32. Photopolymerization profiles of acrylate function of A) **TMPTA** in the presence of **P/Iod** (0.5/2%, w/w) in laminate conditions; and **HEA** in the presence of **P/Iod** (0.5/2%, w/w) B) under air and C) in laminate conditions upon exposure (1) Xe lamp, (2) LED@385 nm, (3) LED@405nm, (4) LED@455 nm, (5) LED@470 nm and (6) LED@530 nm irradiation. Thickness of the film = 25 μm .

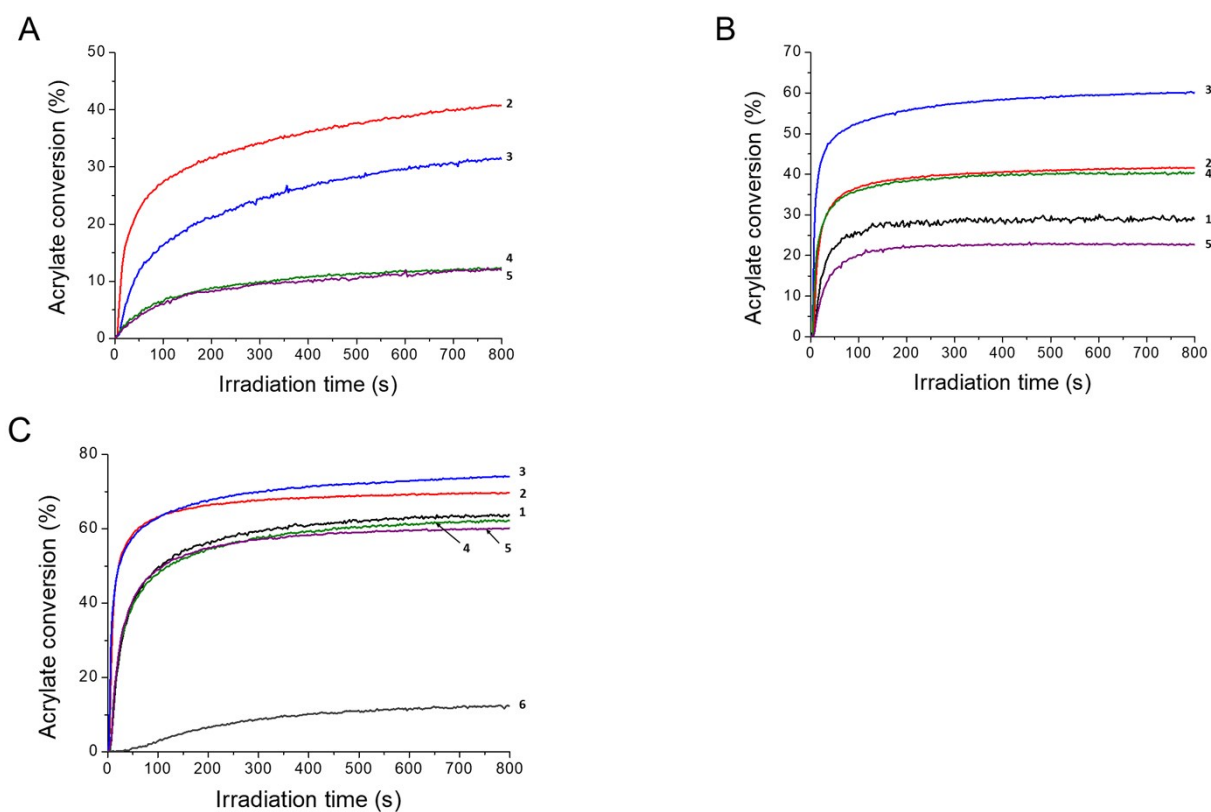


Figure S33. Photopolymerization profiles of acrylate function of **TMPTA** in the presence of (A) **PmA/Iod** (0.5/2%, w/w) in laminate conditions; and **HEA** in the presence of **PmA/Iod** (0.5/2%, w/w) B) under air and C) in laminate conditions upon exposure (1) Xe lamp, (2) LED@385 nm, (3) LED@405nm, (4) LED@455 nm, (5) LED@470 nm and (6) LED@530 nm irradiation. Thickness of the film = 25 μm .

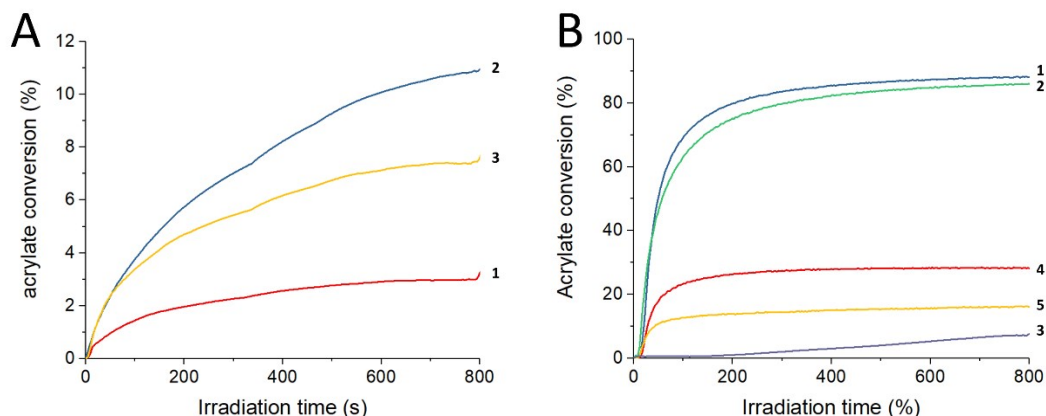


Figure S34. Photopolymerization profiles of acrylate function of A) **TMPTA** in the presence of **BP/Iod** (0.5/2%, w/w) in laminate conditions; and B) **HEA** in the presence of **BP/Iod** (0.5/2%, w/w): in laminate conditions upon exposure (1) LED@385 nm, (2) LED@405nm, and (3) LED@455 nm irradiation; and under air upon exposure (4) LED@385nm and (5) LED@405nm irradiation. Thickness of the film = 25 μm .

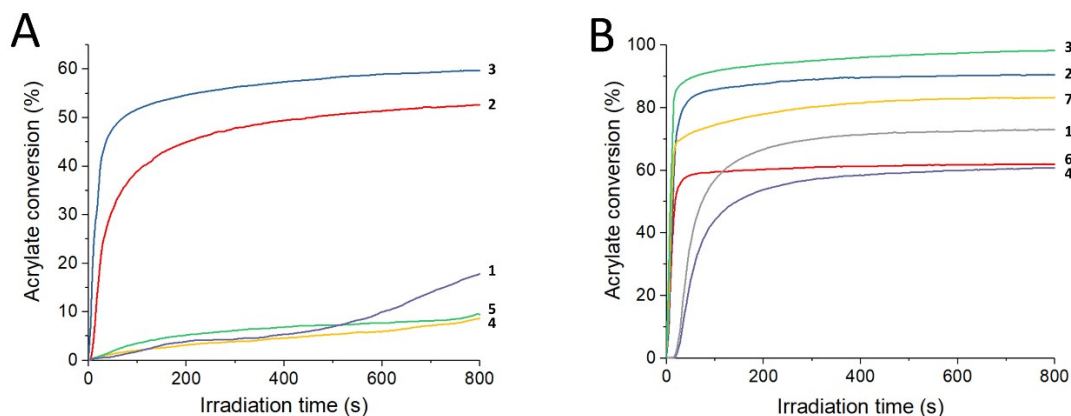


Figure S35. Photopolymerization profiles of acrylate function of A) **TMPTA** in the presence of **AQ/Iod** (0.5/2%, w/w) and B) **HEA** in the presence of **AQ/Iod** (0.5/2%, w/w): in laminate conditions upon exposure (1) Xe lamp, (2) LED@385 nm, (3) LED@405nm, (4) LED@455 nm and (5) LED@470nm irradiation; and under air upon exposure (6) LED@385nm and (7) LED@405nm irradiation. Thickness of the film = 25 μm .

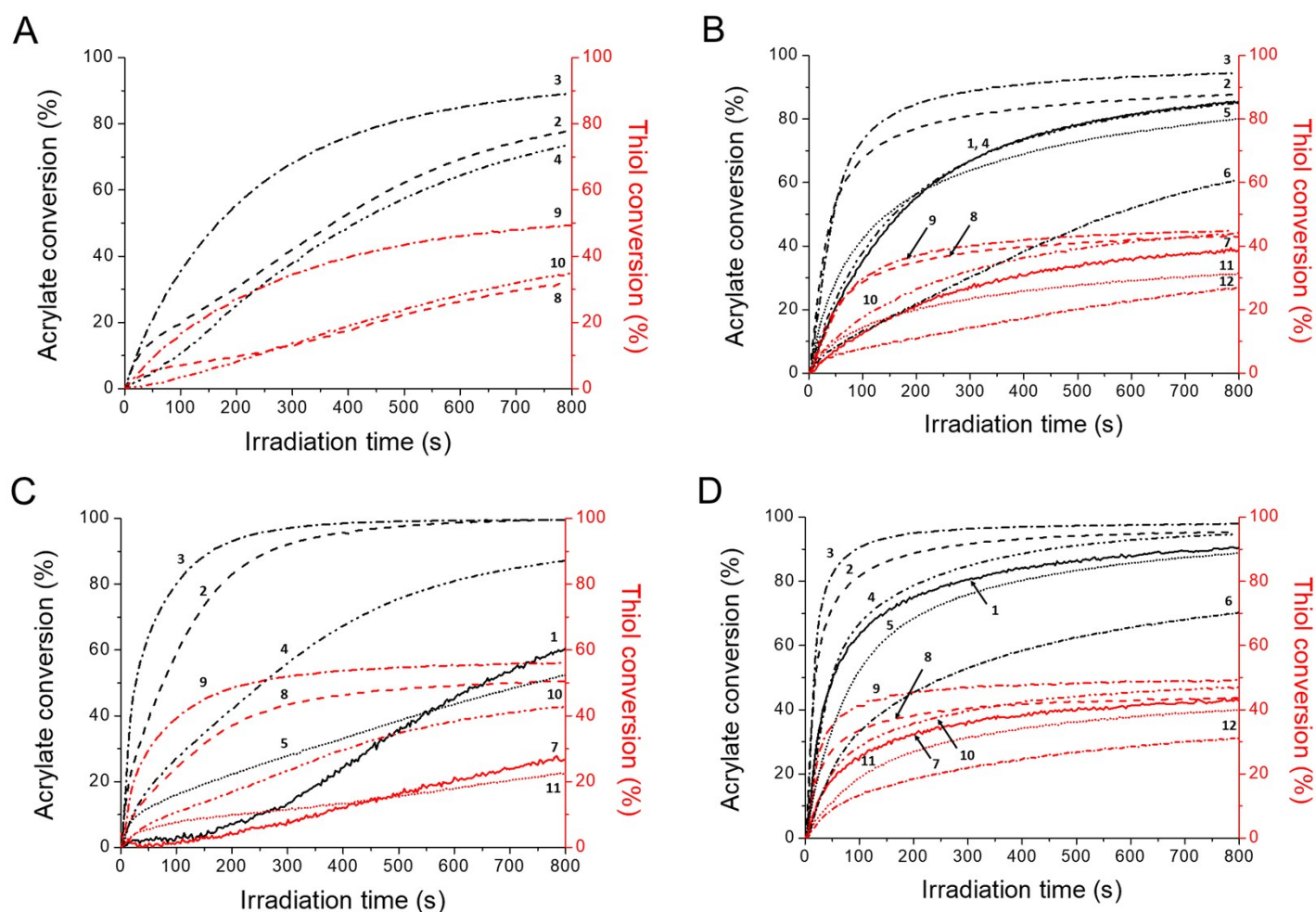


Figure S36. Kinetics profiles of the acrylate and thiol functions in the **TMPTA/TT** (43/57%, w/w) in the presence of **PmA** (0.5 wt%) A) under air and B) in laminate conditions ; and **PmA/Iod** (0.5/2.0%, w/w) C) under air and D) in laminate conditions upon exposure Xe lamp (curves 1 and 7), LED@385 nm (curves 2 and 8), LED@405nm (curves 3 and 9), LED@455 nm (curves 4 and 10), LED@470 nm (curves 5 and 11) and LED@530 nm (curves 6 and 12) irradiation. Curves 1, 2, 3, 4, 5 and 6 = acrylate conversion; curves 7, 8, 9, 10, 11 and 12 = thiol conversion. Thickness of the film = 25 μm .

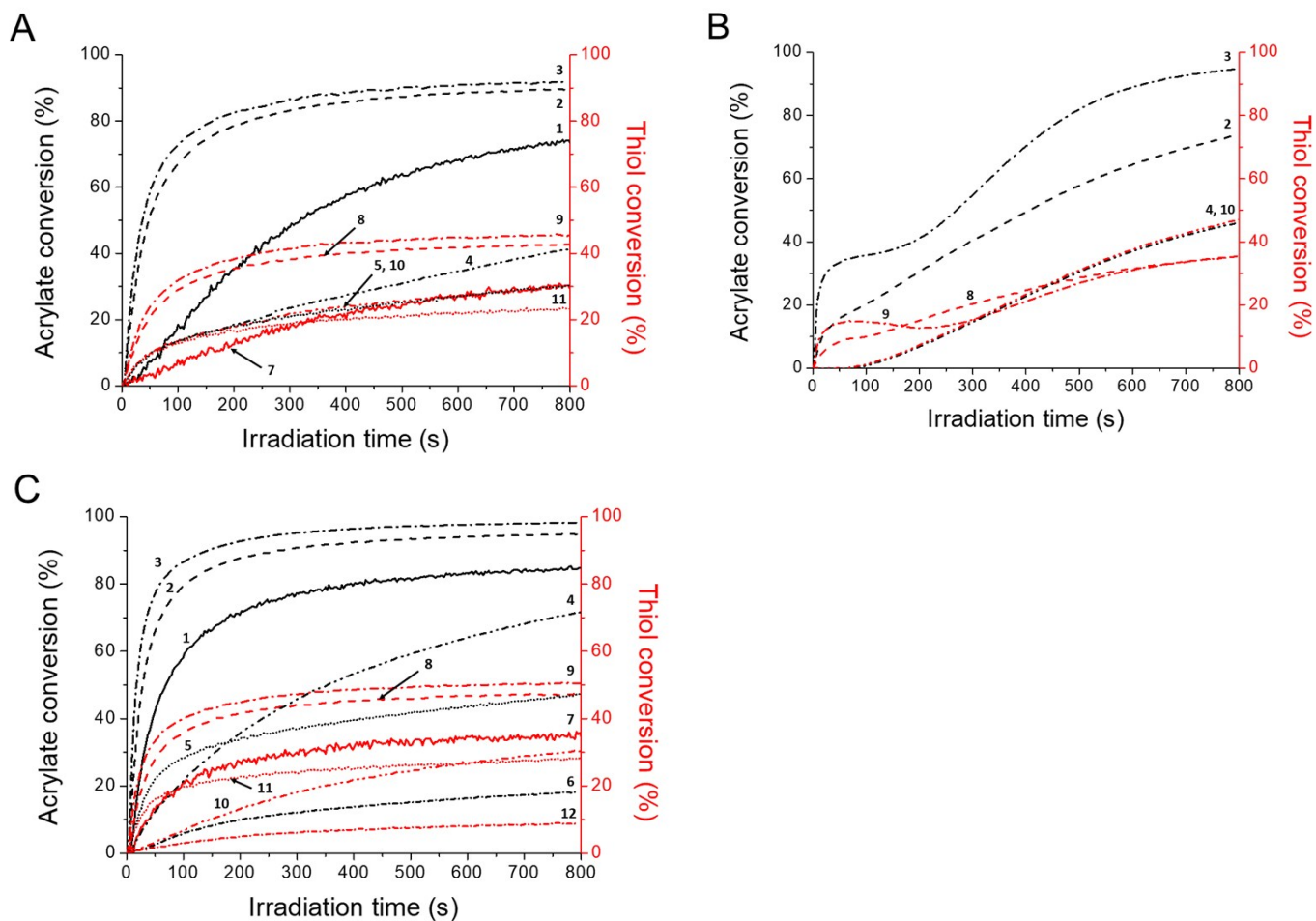


Figure S37. Photopolymerization profiles of a TMPTA/TT blend (43/57%, w/w) in the presence of A) P (0.5 wt%) in laminate conditions; and P/Iod (0.5/2.0%, w/w) B) under air and C) in laminate conditions upon Xe lamp (curves 1 and 7), LED@385 nm (curves 2 and 8), LED@405nm (curves 3 and 9), LED@455 nm (curves 4 and 10), LED@470 nm (curves 5 and 11) and LED@530 nm (curves 6 and 12) irradiation. Curves 1, 2, 3, 4, 5 and 6 = acrylate conversion; curves 7, 8, 9, 10, 11 and 12 = thiol conversion. Thickness of the film = 25 μm .

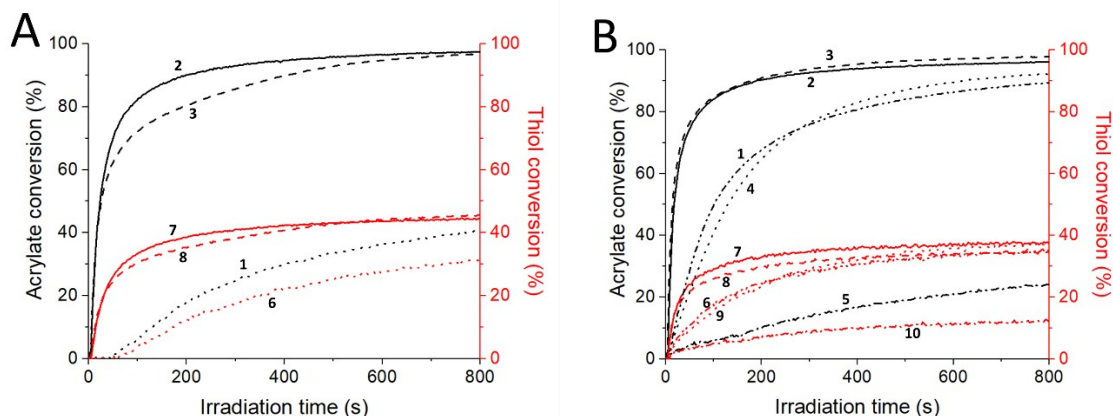


Figure S38. Photopolymerization profiles of a **TMPTA/TT** blend (43/57%, w/w) in the presence of **AQ** (0.5 wt%) A) under air and B) in laminate conditions upon Xe lamp (curves 1 and 6), LED@385 nm (curves 2 and 7), LED@405nm (curves 3 and 8), LED@455 nm (curves 4 and 9) and LED@470 nm (curves 5 and 10) irradiation. Curves 1, 2, 3, 4 and 5 = acrylate conversion; curves 6, 7, 8, 9 and 10 = thiol conversion. Thickness of the film = 25 μm .

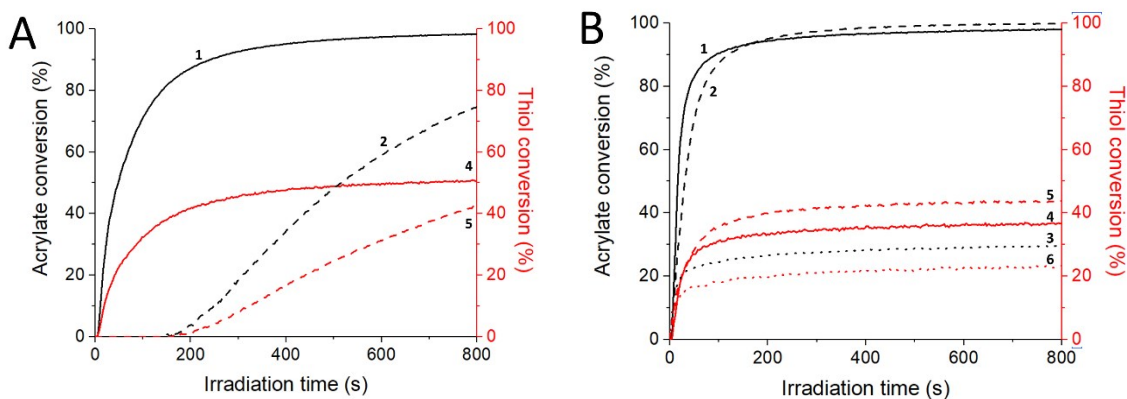


Figure S39. Photopolymerization profiles of a **TMPTA/TT** blend (43/57%, w/w) in the presence of **BP** (0.5 wt%) A) under air and B) in laminate conditions upon LED@385 nm (curves 1 and 4), LED@405nm (curves 2 and 5) and LED@455 nm (curves 3 and 6) irradiation. Curves 1, 2 and 3 = acrylate conversion; curves 4, 5 and 6 = thiol conversion. Thickness of the film = 25 μm .

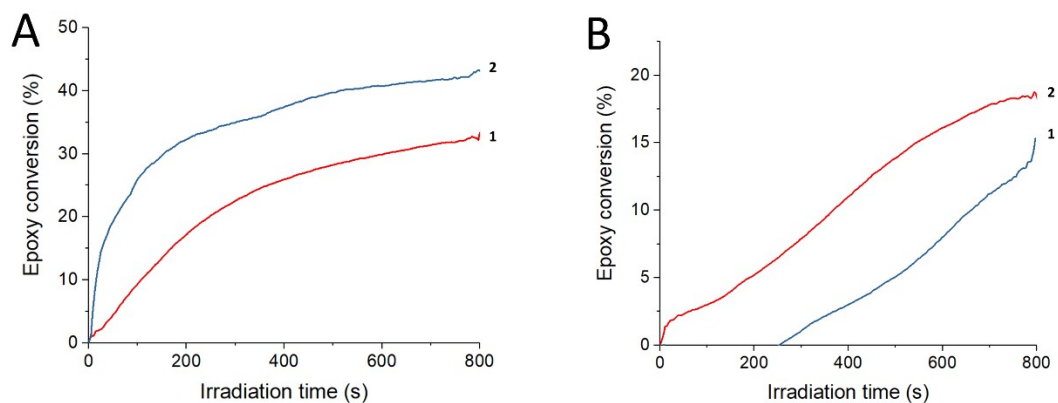


Figure S40. Photopolymerization profiles of epoxy function of EPOX in the presence of (A) **AQ**/Iod (0.5/2%, w/w) and (B) **BP**/Iod (0.5/2%, w/w) under air upon exposure (1) LED@385 nm and (2) LED@405nm irradiation. Thickness of the film = 25 μm .

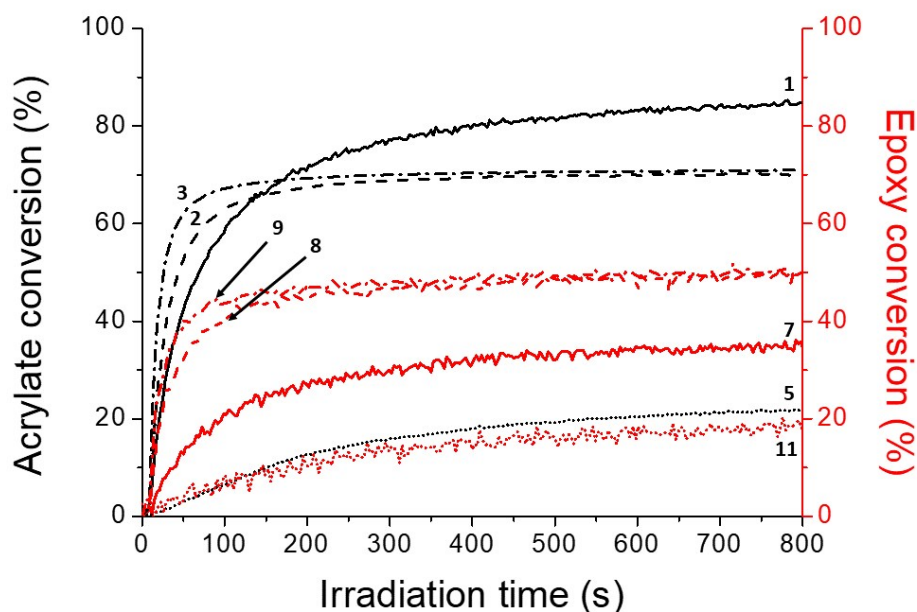


Figure S41. Photopolymerization of a **TMPTA/EPOX** blend (50/50%, w/w) in the presence **P**/Iod (0.5/2.0%, w/w) in laminate conditions upon exposure Xe lamp (curves 1 and 7), LED@385 nm (curves 2 and 8), LED@405nm (curves 3 and 9), LED@455 nm (curves 4 and 10) irradiation. Curves 1, 2, 3 and 5 = acrylate conversion; curves 7, 8, 9 and 11 = thiol conversion. Thickness of the film = 25 μm .

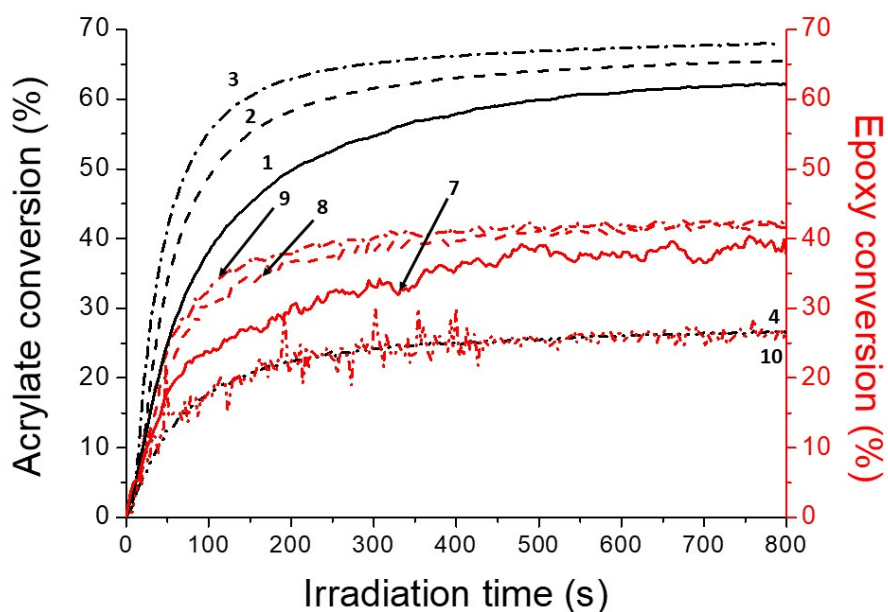


Figure S42. Photopolymerization of a **TMPTA/EPOX** blend (50/50%, w/w) in the presence **PmA/Iod** (0.5/2.0%, w/w) in laminate conditions upon exposure Xe lamp (curves 1 and 7), LED@385 nm (curves 2 and 8), LED@405nm (curves 3 and 9) and LED@455 nm (curves 4 and 10) irradiation. Curves 1, 2, 3 and 4 = acrylate conversion; curves 7, 8, 9 and 10 = thiol conversion. Thickness of the film = 25 μm .

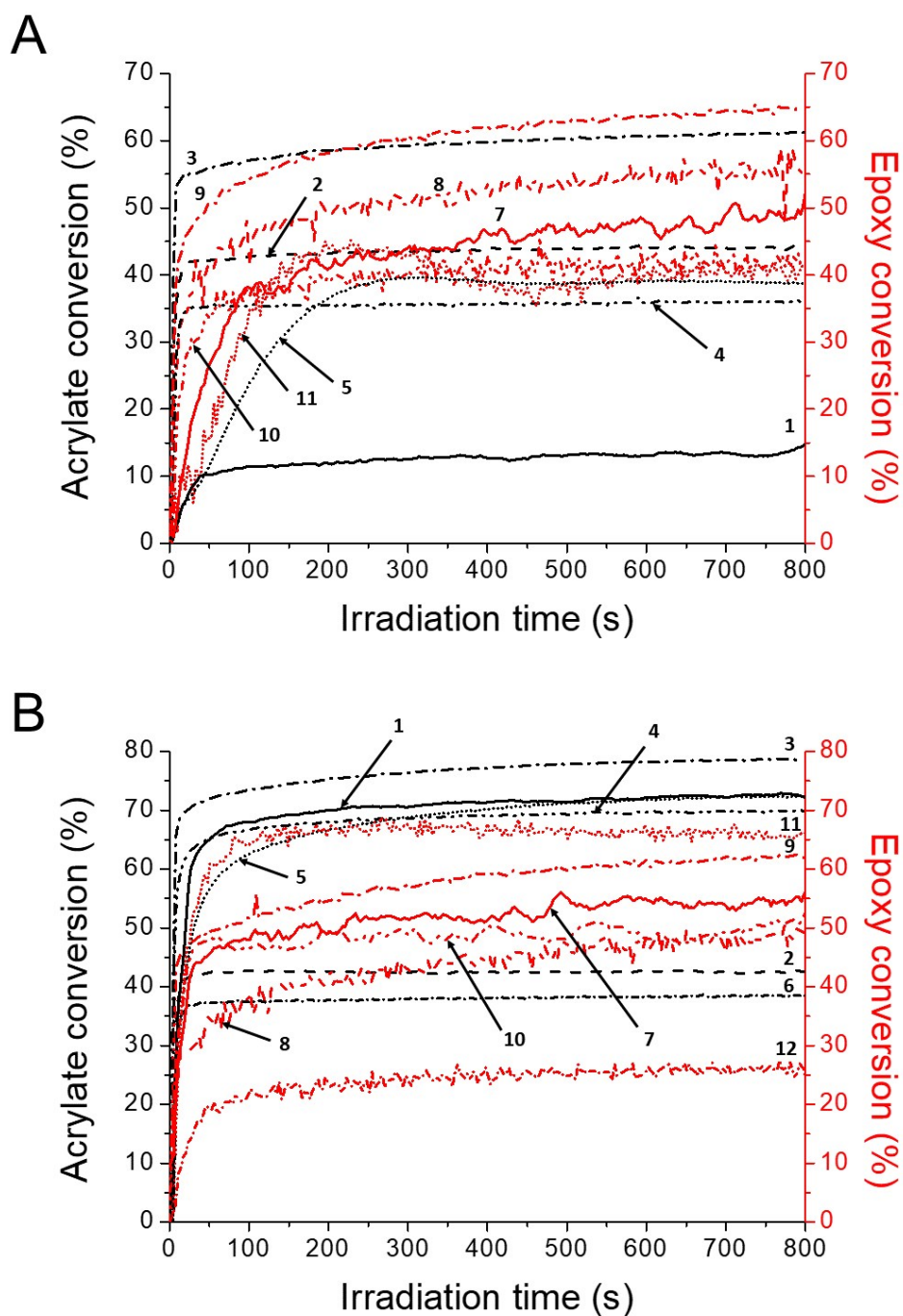


Figure S43. Kinetics profiles of the acrylate and epoxy functions of the **TMPTA/EPOX** blend (50/50%, w/w) in the presence of **PA/Iod** (0.5/2.0%, w/w) A) under air and B) in laminate conditions upon exposure Xe lamp (curves 1 and 7), LED@385 nm (curves 2 and 8), LED@405nm (curves 3 and 9), LED@455 nm (curves 4 and 10), LED@470 nm (curves 5 and

11) and LED@530 nm (curves 6 and 12) irradiation. Curves 1, 2, 3, 4, 5 and 6 = acrylate conversion; curves 7, 8, 9, 10, 11 and 12 = thiol conversion. Thickness of the film = 25 μm .

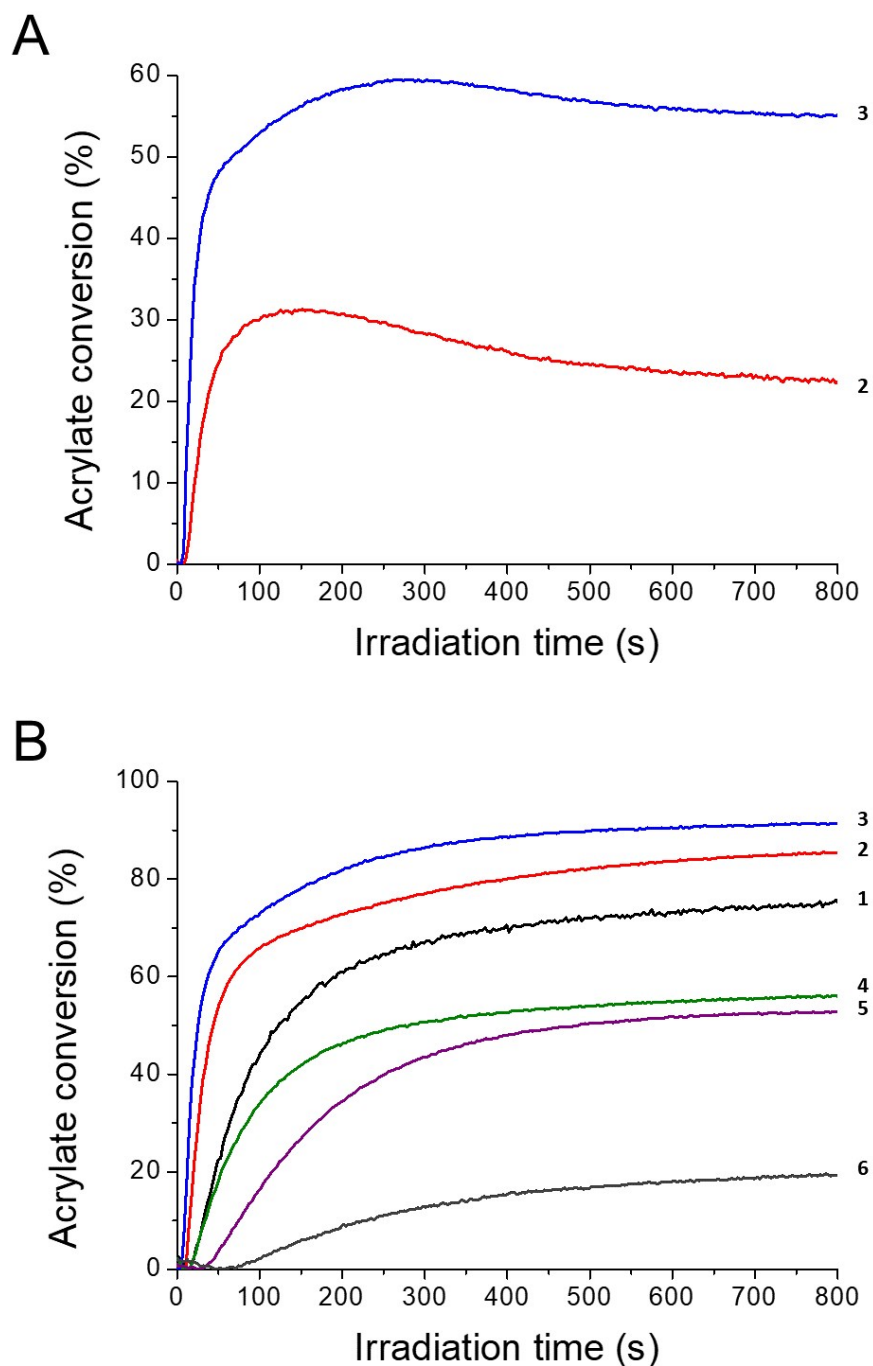


Figure S44. Kinetics profiles of the acrylate functions in the **HEA/EPOX** (50/50%, w/w) in the presence of **P/Iod** (0.5/2.0%, w/w) A) under air and B) in laminate conditions upon exposure

(1) Xe lamp, (2) LED@385 nm, (3) LED@405nm, (4) LED@455 nm, (5) LED@470 nm and (6) LED@530 nm irradiation. Thickness of the film = 25 μm .

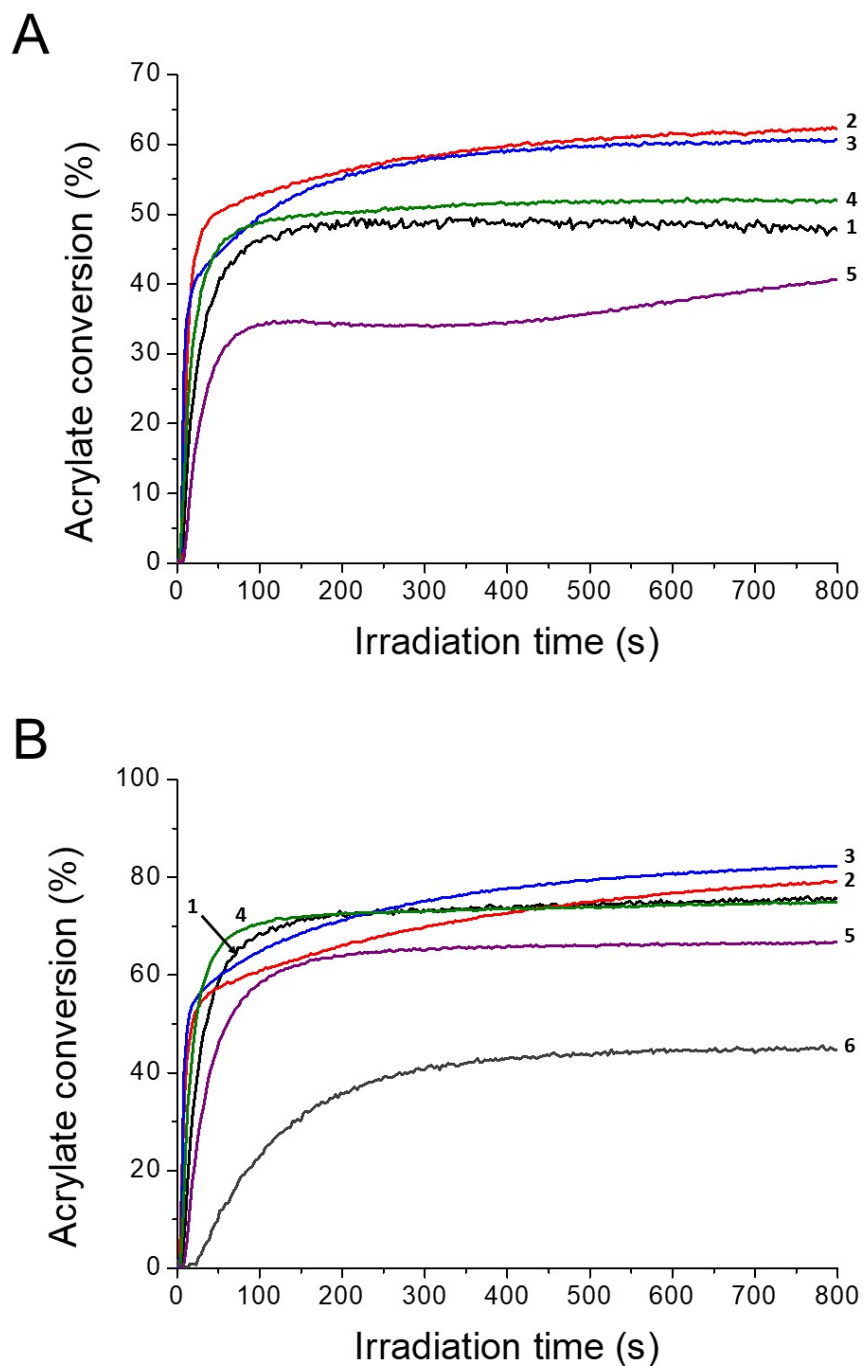


Figure S45. Kinetics profiles of the acrylate functions in the **HEA/EPOX** (50/50%, w/w) in the presence of **PmA/Iod** (0.5/2.0%, w/w) A) under air and B) in laminate conditions upon

exposure (1) Xe lamp, (2) LED@385 nm, (3) LED@405nm, (4) LED@455 nm, (5) LED@470 nm and (6) LED@530 nm irradiation. Thickness of the film = 25 μm .

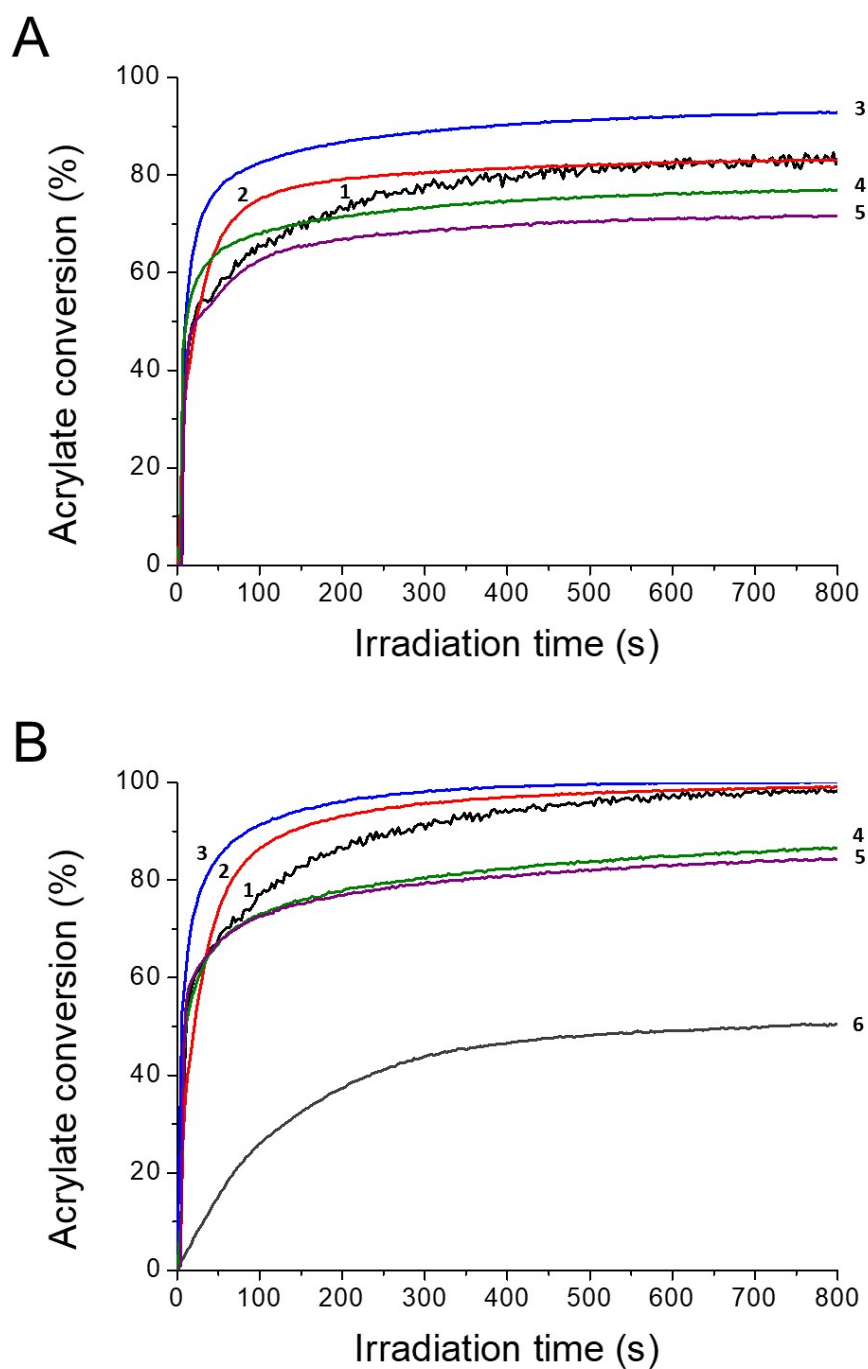


Figure S46. Photopolymerization profiles of a **HEA/EPOX** blend (50/50%, w/w) in the presence of **PA/Iod** (0.5/2.0%, w/w) A) under air and B) in laminate conditions upon exposure (1) Xe lamp, (2) LED@385 nm, (3) LED@405nm, (4) LED@455 nm, (5) LED@470 nm and (6) LED@530 nm irradiation. Thickness of the film = 25 μm .



Figure S47. Optical image of the material used for the antibacterial cycle experiments. Material derived from the photopolymerization of PA/Iod/HEA/EPOX under LED@405 nm for 4 min.

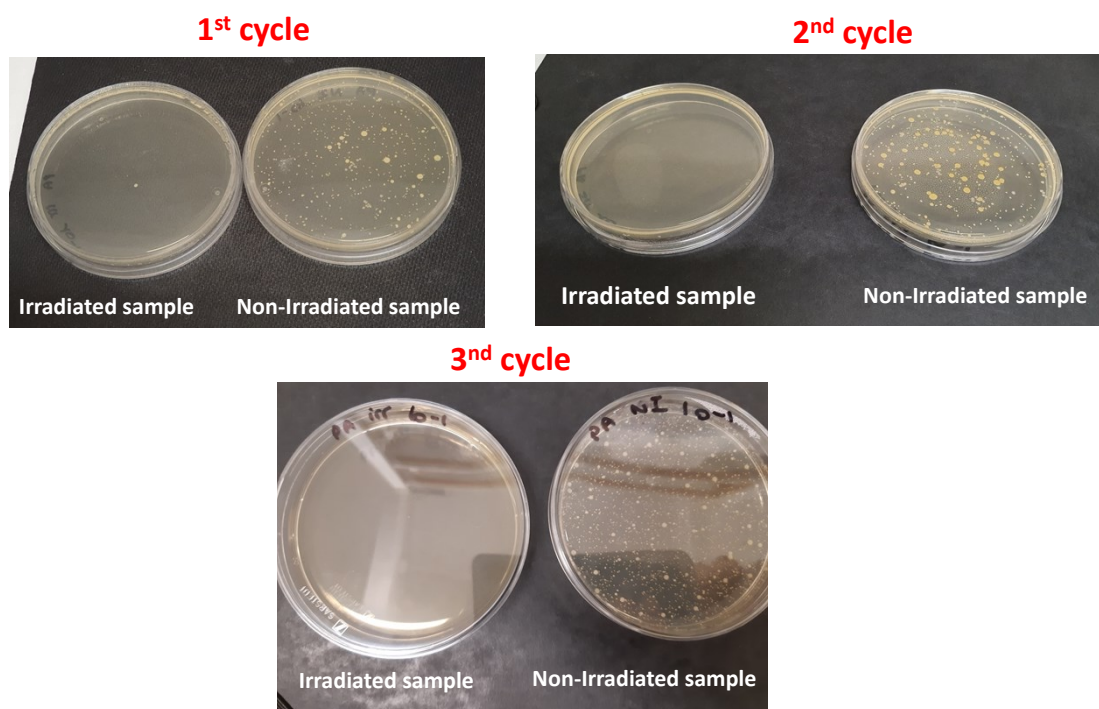


Figure S48. Optical images of the petri dishes of the irradiated and non-irradiated samples for each of the three antibacterial cycle experiments. The small yellow dots in the petri dishes of the non-irradiated samples correspond to *S. aureus* colonies.

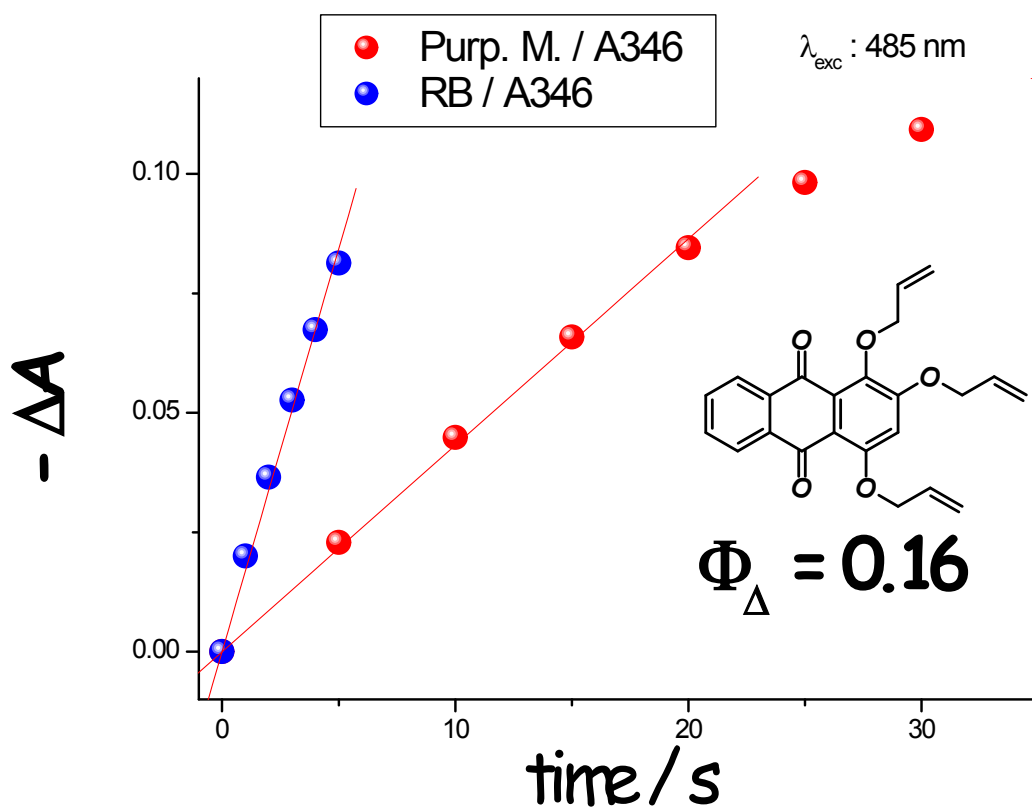


Figure S49. Evaluation of the generated singlet oxygen from the visible-light irradiation of **PA** in ACN (comparison with Rose Bengal). The value of $\Phi_{\text{singlet oxygen (PA)}}/\Phi_{\text{singlet oxygen (RB)}}$ is obtained from the ratio of the corresponding slopes at initial time of irradiation. A value of 0.16 is therefore measured for the $^1\text{O}_2$ photogeneration quantum yield by **PA**.

TABLES

Table S1. Photophysical characteristics of the excited singlet- and triplet-states of **P**, **PmA** and **PA** upon the addition of co-initiators.

	$\lambda_{\text{abs}}^{\text{max}}$ (nm)	$K_{\text{SV}}^{\text{Iod}}$ (M ⁻¹)	$K_{\text{SV}}^{\text{MDEA}}$ (M ⁻¹)	$K_{\text{SV}}^{\text{TT}}$ (M ⁻¹)	$k_{\text{q}}^{\text{Iod}}$ (M ⁻¹ . s ⁻¹)	k_{q}^{ox} (M ⁻¹ . s ⁻¹)	$k_{\text{q}}^{\text{MDEA}}$ (M ⁻¹ . s ⁻¹)	k_{q}^{TT} (M ⁻¹ . s ⁻¹)
P	477	40	4800	-	-	3.4×10^8	-	2.4×10^7
PmA	480	3	13	1	5×10^9	3.7×10^8	2×10^7	-
PA	401	9.5	-	-	1.1×10^8	2×10^8	7×10^8	1.2×10^8

Table S2. The spin-Hamiltonian parameters of phenyl(4-methyl) spin-adduct elucidated from the simulations of the experimental EPR spectra measured upon irradiation of **P**, **PmA** or **PA** in the deoxygenated benzene solutions containing Iod and various spin trapping agents.

Spin trap	a_{N} (mT)	a_{H} (mT)	<i>g</i> -factor
DMPO ^a	1.402±0.003	1.955±0.003	2.0060±0.0001
PBN ^b	1.452±0.003	0.221±0.0006	2.0061±0.0001
PBN (¹⁵ N)	2.106±0.003	0.293±0.003	2.0061±0.0001
ND	1.027±0.002	0.093±0.001, 0.093±0.001(H ^{meta}) 0.287±0.002, 0.270±0.001 (H ^{ortho}) 0.308±0.001, 0.308±0.001, 0.305±0.001 (CH ₃) ^{para}	2.0059±0.0001

^a ¹³C satellites 0.781 mT (2×¹³C), 0.580 mT, 0.552 mT ; ^b ¹³C satellites 0.749 mT (2×¹³C), 0.492 mT (4×¹³C)²⁴

Table S3. The spin-Hamiltonian parameters of anthrasemiquinones estimated from the simulations of the experimental EPR spectra measured upon irradiation of **P**, **PmA** (LED@450 nm) or **PA** (LED@400 nm) in the deoxygenated benzene solutions containing MDEA.

Photosensitizer	a_{H} (mT)	<i>g</i> -factor
P	not resolved	2.0043±0.0001
PmA	0.130 (2H), 0.124 (1H), 0.074 (2H), 0.062 (2H)	2.0040±0.0001
PA	0.174 (1H), 0.114 (1H), 0.106 (2H), 0.066 (1H)	2.0041±0.0001